Identifying complex Fermi resonances in *p*-difluorobenzene using zero-electron-kinetic-energy (ZEKE) spectroscopy

David J. Kemp, Adrian M. Gardner,[a] William D. Tuttle, Jonathan Midgley, Katharine L. Reid and Timothy G. Wright*

School of Chemistry, University of Nottingham, University Park, Nottingham, NG7 2RD, U.K.

a) Present Address: Stephenson Institute for Renewable Energy, University of Liverpool, L69 7ZF, UK

*To whom correspondence should be addressed. Email: Tim.Wright@nottingham.ac.uk

Abstract

The vibrations of the ground state cation ($\tilde{X}^2B_{2g}$) of *para*-difluorobenzene (*p*DFB) have been investigated using zero-electron-kinetic-energy (ZEKE) spectroscopy. A comprehensive set of ZEKE spectra were recorded via different vibrational levels of the S_1 state (< 0^0 + 1300 cm^{-1}). The adiabatic ionization energy (AIE) for *p*DFB was measured as 73869±5 cm^{-1}. Use of different intermediate levels allows different cationic vibrational activity to be obtained via the modification of the Franck-Condon factors for the ionization step, allowing the wavenumbers of different vibrational levels in the cation to be established. In addition, assignment of the vibrational structure in the ZEKE spectra allowed interrogation of the assignments of the $S_1 \leftarrow S_0$ transition put forward by Knight and Kable [A. E. W. Knight and S. H. Kable, J. Chem. Phys. **89**, 7139 (1988)]. Assignment of the vibrational structure has been aided by quantum chemical calculations. In this way it was possible to assign seventeen of the thirty vibrational modes of the ground state *p*DFB^+ cation. Evidence for complex Fermi resonances in the S_1 state, i.e. those that involve more than two vibrations, was established. One of these was investigated using picosecond time-resolved photoelectron spectroscopy. In addition, we discuss the appearance of several symmetry-forbidden bands in the ZEKE spectra, attributing their appearance to a Rydberg state variation of an intrachannel vibronic coupling mechanism.

I. INTRODUCTION

The *p*-difluorobenzene (*p*DFB) molecule is a prototypical D_{2h} point-group symmetry molecule and is a useful probe of the effect of a symmetric *para* disubstitution on the π-orbital system of the D_{6h} symmetry benzene molecule. The outermost electronic configuration is $\ldots b_{3u}^2 b_{1g}^2 b_{2g}^2 a_u^0$ for *p*DFB and so it may thus be seen that the lowest energy $a_u \leftarrow b_{2g}$ excitation gives rise to the $\tilde{A}^1B_{2u}$ electronic state (denoted S_1), and the lowest-energy ionization yields the $\tilde{X}\ ^2B_{2g}$ ground state cation (denoted D_0^+).

The $S_1 \leftarrow S_0$ transition has been studied in depth by Cooper[1], Robey and Schlag (RS),[2] Coveleskie and Parmenter (CP),[3] and particularly by Knight and Kable (KK).[4] Cooper's study[1] was via one-photon absorption, with vibrational progressions being identified and assignments to some totally-symmetric modes being made. RS[2] employed two-photon absorption spectroscopy of a room-temperature gaseous sample, using both linearly- and circularly-polarized light. CP[3] and KK[4] each used laser-induced fluorescence (LIF), with the assignments also being interrogated by dispersed fluorescence (DF), with CP employing a room temperature gaseous sample, and KK using a jet-cooled sample. As a result of these studies, many of the S_1 vibrational wavenumbers have been established. The KK study[4] has the most comprehensive set of S_1 vibrational wavenumbers, which are summarized in Table 1, where several values are in poor agreement with the calculated values. Parmenter and coworkers have also studied *p*DFB with a view to comparing to the behaviour of *para*-fluorotoluene (*p*FT) in investigations of the effect on intramolecular vibrational redistribution (IVR) caused by a methyl group – see for example, Ref. 5.

The photoelectron spectrum of *p*DFB has been reported by a number of workers, with laser-based photoelectron spectroscopy (PES) studies including the REMPI-PES studies of Sekreta et al.[6] and Bellm and Reid,[7] and the zero-electron-kinetic-energy (ZEKE) study of Müller-Dethlefs and coworkers.[8,9] In addition, there are two-colour mass-analyzed threshold ionization (MATI) spectra from Lembach and Brutschy[10], recorded as part of their study of vibrational predissociation in the *p*DFB-Ar complex. Finally, a one-photon MATI study by Kwon et al. [11] has been reported, where the ionization occurs directly from the neutral ground state, S_0. These studies have provided wavenumber values for a number of the ground state cation vibrations, which are summarized in Table 1. A number of these values are in disagreement, and there is still uncertainty regarding some of the assignments. We note that: the REMPI-PES studies of Sekreta et al.[6] and Bellm and Reid[7] suffer from reduced resolution compared to the other studies; the ZEKE and MATI studies of Reiser et al.[9] and Lembach and Brutschy[10]

employ only a limited number of intermediate levels; and the MATI study of Kwon et al.[11] is limited by the fact that it is a single-photon method, and so resonant intermediate levels cannot be employed in order to vary the Franck-Condon activity – i.e. just a single MATI spectrum is obtained from the S_0 vibrationless level. It is the aim of the present work to carry out a comprehensive study of the S_1 vibrational levels by recording ZEKE spectra via all significant intermediate levels observed in the $S_1 \leftarrow S_0$ excitation, below 1300 cm^{-1}. This will allow significant variation of the Franck-Condon factors for the ionization step to be achieved. Further, comparison of the observed activity following projection of the population of the S_1 state onto the ground state neutral (DF in Ref. 4) and cation (ZEKE, this work) levels should provide further evidence for the assignments, particularly the occurrence of Fermi resonances.

Information on the ground state cation and its excited states has been obtained by Bondybey et al. by electronic absorption spectroscopy in an inert matrix,[12] and by Ito and coworkers[13,14] via a variant of two-colour REMPI spectroscopy, termed mass-selected ion-dip spectroscopy. Further, complete-active space calculations including second-order perturbative treatment of dynamic electron correlation (CASPT2) on the low-lying electronic states of the *p*DFB cation have been reported by Yu and Huang.[15]

We shall also report time-resolved photoelectron spectra using picosecond laser pulses, with which vibrational resolution can be achieved.[16,17,18]

II. EXPERIMENTAL

The REMPI and ZEKE apparatus employed has been described previously in detail elsewhere.[19, 20] The *p*DFB vapour above a room temperature sample was seeded in ~1.5 bar of Ar and the gaseous mixture passed through a General Valve pulsed nozzle (750 μm, 10 Hz, opening time of 180–210 μs) to create a free jet expansion. The excitation and ionization sources were dye lasers (Sirah Cobra-Stretch) operating with C540A or C503, depending on the energetic region of interest. The two dye lasers were pumped by either a Surelite I or Surelite III Nd:YAG laser, which varied in different experiments. The third harmonic (355 nm) was used to pump the dye lasers, and their fundamental frequencies were frequency doubled using BBO crystals. These frequency-doubled outputs were focused and overlapped temporally and spatially – coaxially and counterpropagating – in the centre of a vacuum chamber. Here, they intersected the free jet expansion between two biased electrical grids located in the extraction region of a time-of-flight mass spectrometer, which was employed in the REMPI

experiments. These grids were also used in the ZEKE experiments by application of pulsed voltages, giving typical fields (F) of ~10 V cm^{-1}, after a delay of up to 2 μs, where this delay was minimized while avoiding the introduction of excess noise from the prompt electron signal. ZEKE bands had widths of ~5-7 cm^{-1}, even when $\sqrt{F}$ relationships would suggest the widths should be significantly greater, because of the well-known decay of the lower-lying Rydberg states accessed in the pulsed-field ionization process.[21] Where possible, we excited in the "dip" in the centre of a REMPI band, which should correspond to the lowest rotational energy levels, and so produce narrow ZEKE bands.

The picosecond time-resolved photoelectron imaging apparatus has been described previously,[22] and a study of the higher-wavenumber $5^1 9^1$ bands in *p*DFB has been reported.[23] In brief, two independently tuneable, vertically-polarized UV laser beams were produced from the frequency-doubled outputs of two optical paramagnetic amplifiers (Light Conversion), pumped by a picosecond Ti:Sapph laser system (Coherent). A UV pulse duration of 1 ps, corresponding to a bandwidth of 13 cm^{-1}, was employed for both pump and probe. One of these UV outputs prepared a wavepacket in the S_1 state by the coherent excitation of a superposition of eigenstates, and then the second, spatially overlapped and counterpropagating, ionized the evolving superposition after a variable time delay (-20 to +250 ps), which was controlled by a motorized delay stage (Standa). Photoelectron images were obtained using a velocity-map imaging spectrometer,[7] and the time-resolved spectra were obtained from the measured images.[24]

III. RESULTS AND DISCUSSION

In Table 1 we show calculated wavenumbers for *p*DFB in the S_0, S_1 and D_0^+ states; in addition, we have also included the experimental values, where available – a number of which are established or confirmed in the present work. The experimental and calculated wavenumbers for the S_0 state are discussed in depth in Ref. 25. The calculated wavenumbers for the S_1 and D_0^+ states are taken from Refs. 26 and 27, where comparisons were made to available experimental values and those of the vibrations of *p*FT and *para*-xylene (*p*Xyl). In the present work we shall discuss some of the S_0 and S_1 assignments in the light of the ZEKE spectra including the identification of Fermi resonances, via the activities of vibrations in the D_0^+ state.

A. REMPI Spectrum

In Figure 1, we show the REMPI spectrum of *p*DFB in the range 0–1300 cm^{-1}. The spectrum has been calibrated to agree with the absorption spectrum presented by Cvitaš and Hollas[28], with the $S_1 0^0$ origin wavenumber at 36837.9 cm^{-1}. The REMPI spectrum is not normalized to the UV intensity, but looks very similar to the corresponding portion of the LIF spectrum presented in Ref. 4, both with regard to band positions and relative intensities. It is notable that the origin and a number of totally-symmetric vibrations, such as 11^1, 9^1 and 5^1 are significant contributors. The assignments given in Figure 1 are discussed below, where expanded views of some sections of the spectrum are presented.

Since there are a large number of ZEKE spectra to discuss, we split these into groups according to their energetic proximity and activity. In each case, we shall also discuss the assignments in the light of the DF spectra of KK.[4] In previous work, we have also highlighted the correspondence in vibrational activity for REMPI and ZEKE spectra of similar molecules,[29] if a consistent labelling scheme for the vibrations is employed; hence, the D_i labels of Ref. 25 are employed in the present study, and the forms of the vibrations, and further discussion, can be found in that work. In earlier work, both Mulliken[30]/Herzberg[31] and Wilson[32]/Varsányi[33] labels have been employed. In referring to previous studies, we will also employ the D_i labels of Ref. 25, and to aid the reader the correspondence between the different labels are given in Table 1.

Note that almost all transitions will commence from the S_0 zero-point level for our jet-cooled sample, and so the lower vibrational level is omitted when denoting transitions. (For succinctness, we shall often refer to a "level" by using the notation of a transition – in such cases the "level" refers to the upper one of the transition.) An exception is hot bands (marked with red dots in Figure 1), where we will explicitly indicate the lower level for clarity. Thus, in Figure 1, we can see that there is a persistent vibrational hot band at -100 cm^{-1}, which may be assigned to the 19_1^1 transition in agreement with Cvitaš and Hollas[28]; this band is rotationally cold, as judged by its narrowness, but interestingly it is difficult to cool out this vibrational hot band feature associated with the D_{19} vibration. There are also weaker features at -36 cm^{-1} and -41 cm^{-1}, which may be assigned to 20_1^1 and 11_1^1, with the former assignment in agreement with CP;[3] it is also possible there is a contribution from *p*DFB-Ar to these latter features. We shall see that the more-intense 19_1^1 transition is responsible for the presence of

other hot bands seen in the REMPI spectrum, which we shall highlight below. No clear evidence has been found of contributions related to the other hot band features.

In the ZEKE spectra the assignments of the most intense, and other pertinent bands are indicated; however, we refrain from labelling every single weak band, many of which appear more intensely in other spectra.

B. ZEKE spectra via S_1 0^0 and "accidental" resonances

In Figure 2(a), we show a ZEKE spectrum recorded via the S_1 origin transition, 0^0. Corresponding ZEKE spectra were presented in Refs. 8 and 9 and are similar in appearance, but we present a more expanded version here; in addition, our ZEKE spectrum looks similar to the limited range reported in the corresponding MATI spectrum of Lembach and Brutschy.[10] The assignments are relatively straightforward, based on previous work[6,8,9,10,11] and quantum chemical calculations of the vibrational wavenumbers in the D_0^+ state[26] (see Table 1). We see the expected dominance of the $\Delta v = 0$ band, accompanied by other totally-symmetric activity, such as the totally-symmetric (a_g) fundamental bands 11^1, 9^1, 7^1, 5^1 and 3^1. The position of the origin allows the adiabatic ionization energy to be determined as 73869±5 cm^{-1}, which is a little higher than that of Kwon et al.[11] (73861 ± 5 cm^{-1}), but in excellent agreement with those of Fujii et al.[34] (73871 cm^{-1}) and Rieger et al.[8] (73872 ± 3 cm^{-1}). Interestingly, to low wavenumber three non-totally-symmetric fundamental bands are observed, corresponding to 20^1, 19^1 and 14^1, with the terminating levels having b_{3u}, b_{2g}, and a_u symmetry, respectively. One explanation for their appearance is vibronic coupling[9] – we shall discuss the appearance of these, and other such bands in Section IV.B.2 In other spectra, to be discussed below, it will be seen that many of the assigned bands in Figure 2(a) appear again, although with different relative intensities; in addition, a number of other bands appear which are not present in the spectrum in Figure 2(a), showing the utility of recording ZEKE spectra via different intermediate levels.

When recording ZEKE spectra, features arise that are not two-colour in origin and so are not part of the actual $D_0^+ \leftarrow S_1$ ZEKE spectrum. In Refs. 8 and 9 such signals were attributed to "trapped" electrons, but in recent work on *para*-chlorofluorobenzene (*p*ClFB)[35] we established that a key aspect regarding the appearance of these spurious signals is two-photon, one-colour "accidental resonance" in both the S_1 and D_0^+ states. It was pointed out that the positions of these accidental resonances are coincident with REMPI bands, but the intensities were different – giving an indication of their double resonance character. An accidental resonance signal will be produced if the two-photon energy takes

the molecule to high-lying Rydberg states just below an ionization threshold, which are then field-ionized by the pulsed-field extraction, in the usual way as for ZEKE spectroscopy. Alternatively, a signal could also arise when the two-photon energy is just above threshold, if the number of ions present at the laser focus is sufficient to "trap" these slow electrons – this is the suggested mechanism in Refs. 8 and 9. In both cases, we expect a narrow band, since the production of the high-lying Rydberg states (or slow electrons) can only occur across a narrow wavenumber range when the laser is also resonant with a $S_1 \leftarrow S_0$ transition. These one-colour accidental resonance signals appear across the ZEKE spectra, and are labelled with an asterisk in each case. Of course, achieving resonance for a second photon being absorbed becomes more likely at higher energies, since higher vibrational levels in the cation are being accessed, where the density of states is higher.

A second, but related, two-colour mechanism also occurs. In these cases, the scanning "ionization" laser in the ZEKE experiment becomes resonant with the energy of an $S_1 \leftarrow S_0$ transition and, additionally, the fixed "excitation" laser is then accidentally resonant with a transition from this S_1 level, to a level in the cation. This then leads to the production of high-lying Rydberg states (or perhaps slow electrons), as noted above. These signals are labelled with an obelus (†) in the ZEKE spectra, but we refrain from assigning all of these resonances in detail; however, will comment on several notable ones in the following text – the interested reader can also refer to Ref. 35 to see a discussion of some such resonances in *p*ClFB.

In the present case of *p*DFB, we found that the relative intensities of the accidental resonance bands, particularly the one-colour ones, were very dependent on the day-to-day conditions, although they appeared at the same wavenumbers. This may point to these features being associated more with trapped electrons for *p*DFB, produced just above threshold, than high-lying Rydberg states – in agreement with the suggestion in Refs. 8 and 9.

C. ZEKE spectra via the overtone features $S_1\,20^2$ and $S_1\,14^2$

The ZEKE spectra via the 20^2 and 14^2 transitions are shown in Figure 2(b) and (c) and are reported here for the first time; each can be seen to be dominated by the $\Delta v = 0$ band. Also present in the regions scanned are the 11^1X^2 combination bands and, in the case of 20^2, also the 9^120^2 combination band. Interestingly, the 0^0 and 11^1 bands are both reasonably intense in the case of the 14^2 spectrum, but are absent for 20^2, even though they are Franck-Condon allowed in each case. Via $S_1\,14^2$, we also see two of the symmetry-forbidden bands, 19^1 and 14^1 (but not 20^1) that were seen via the origin, but only

20^1 is seen when exciting via $S_1\,20^2$, suggesting different vibronic activity. Notably the strongest non-Franck-Condon bands in each case correspond to $\Delta v = \pm 1$.

A weak feature at 311 cm^{-1} is also seen in the REMPI spectrum that was tentatively assigned to 14^120^1 by KK, but we note that this is not consistent with the 20^2 and 14^2 band positions. KK did not record a DF spectrum. In fact, we are convinced that this REMPI feature is in fact a hot band corresponding to the transition $11_0^1 19_1^1$ and is the counterpart of the persistent hot band that appears at -100 cm^{-1}, discussed earlier in Section III.A. We managed to record a weak ZEKE spectrum via this feature consistent with this assignment.

In Ref. 9, a ZEKE spectrum via the 20^1 level in S_1 was recorded, accessed via the hot band transition, 20_1^1, providing a wavenumber for D_{20} in the cation in good agreement with the present value (see Table 1), and consistent with the position of the 20^1 ZEKE band observed in other spectra reported herein.

The above assignments agree with those of KK.[4]

D. ZEKE spectra recorded via the fundamentals $S_1\,29^1$ and $S_1\,11^1$

These two bands lie close to each other in the REMPI spectrum at 401 cm^{-1} and 411 cm^{-1} (see Figure 1). The vibrations are of different symmetries, being b_{3g} and a_g, respectively; the former is vibronically induced by Herzberg-Teller coupling,[4] while the latter is Franck-Condon allowed, although its intensity could also be affected by Herzberg-Teller coupling.[36] The ZEKE spectra obtained are shown in Figure 2(d) and (e). ZEKE spectra via both of these levels were reported in Ref. 9, and our spectra are consistent with those.

The ZEKE spectrum recorded via 29^1 may be seen to be dominated by the $\Delta v = 0$ band, with the expected 11^129^1 and 9^129^1 combination bands to higher wavenumber, as well as the vibronically-induced 20^129^1, 19^129^1 and 14^129^1 bands. The 0^0 band is absent in line with Franck-Condon expectations.

On the other hand, the activity in the ZEKE spectrum recorded via 11^1 is very different. Immediately apparent is that is not the $\Delta v = 0$ band, but the $\Delta v = +1$ band, 11^2, that is the most intense, with

significant intensities also in 0^0 (Δv = -1) and 11^3 (Δv = +2). We also see the weak vibronically-induced bands 20^1 (barely discernible in the figure), 19^1 and 14^1, as well as: the 18^1 band (not reported in Refs. 9 or 10); a weak band corresponding to 28^1. There are also a number of other bands corresponding to totally-symmetric vibrations, as expected. Overall, it is interesting that these two spectra are mutually exclusive in terms of activity, owing to the difference in the symmetries of the intermediate levels, even though these only lie 10 cm^{-1} apart.

Both of these assignments agree with those of KK.[4]

E. ZEKE spectra recorded via bands in the region 540–800 cm^{-1}

We first discuss three REMPI bands that appear in the lower wavenumber part of this region, at 545 cm^{-1}, 558 cm^{-1} and 652 cm^{-1}. ZEKE spectra via each of these features can be seen in Figure 3(a)–(c) and are reported here for the first time.

The ZEKE spectrum via the 545 cm^{-1} level – Figure 3(a) – is consistent with the assignment of the REMPI band as 19^2, with the Δv = 0 band at 613 cm^{-1} in the ZEKE spectrum; this is also consistent with the assignment by KK.[4] There is some similarity of the appearance of the spectrum to that of the 20^2 spectrum shown in Figure 2(b), with the Δv = ±1 bands being seen, as well as the vibronically-induced 14^119^2 band; unfortunately, it was not quite possible to scan as far as the 0^0 band with the laser dyes employed. In Ref. 9, a ZEKE spectrum was recorded via the 19^1 level, accessed via the hot band transition, 19^1_1, which gave a value for D_{19} in the cation in good agreement with the present value (see Table 1) and also obtained via other spectra herein. It can be seen that there are two strong two-colour accidental resonances (cf. Section III.B) in the ZEKE spectrum at 357 cm^{-1} and 714 cm^{-1}, which may be assigned, respectively, as:

$$D_0^+ 14^1 \leftarrow S_1 0^0 \leftarrow S_0$$

$$D_0^+ 14^2 \leftarrow S_1 14^2 \leftarrow S_0$$

The ZEKE spectrum recorded via the 558 cm^{-1} level – Figure 3(b) – shows a strong band at 584 cm^{-1}, allowing the S_1 level to be assigned to the transition involving the vibronically active b_{3g} vibration D_{28}. We also see the expected combination band, 11^128^1 to higher wavenumber. The assignment of the S_1

level to 28^1 agrees with the assignment of KK,[4] and the ZEKE spectrum firmly establishes the wavenumber for this vibration in both the S_1 and D_0^+ states. A two-colour accidental resonance band (cf. Section III.B) appears at 729 cm^{-1}, which corresponds to one of the resonances seen via the 545 cm^{-1} level, but now at a different apparent wavenumber:

$$D_0^+ 14^2 \leftarrow S_1 14^2 \leftarrow S_0$$

The ZEKE spectrum recorded via the 652 cm^{-1} feature – Figure 3(c) – confirms KK's[4] assignment of the S_1 level to 11^120^2, with both the Δv = 0 and 11^220^2 bands observed. There are several one-colour accidental resonances in this region, plus three two-colour ones (cf. Section III.B). The latter are at 861 cm^{-1}, 871 cm^{-1} and 1017 cm^{-1}, and may be assigned, respectively, as:

$$D_0^+ 11^129^1 \leftarrow S_1 29^1 \leftarrow S_0$$

$$D_0^+ 11^2 \leftarrow S_1 11^1 \leftarrow S_0$$

$$D_0^+ 11^128^1 \leftarrow S_1 28^1 \leftarrow S_0$$

We now move onto the REMPI features to higher wavenumber. First, we note that the transition corresponding to the REMPI band at 704 cm^{-1} was assigned as 30^2 by KK[4] on the basis of the S_1 wavenumber of the fundamental from RS,[2] but this was not confirmed by recording DF spectra. The band at 719 cm^{-1} was unassigned by KK. We have attempted to record ZEKE spectra via both of these features. When exciting via the 704 cm^{-1} feature, only very weak ZEKE features could be obtained (spectrum not shown), and none of those was at the correct wavenumber for the Δv= 0 band of 30^2. As such, the assignment of the 704 cm^{-1} band must remain tentative. When exciting via the 719 cm^{-1} REMPI band, we did obtain a ZEKE spectrum with reasonable signal-to-noise (not shown); however, it became apparent that the spectrum looked very similar to that obtained via the 9^1 REMPI band, hence this, and its wavenumber, established the assignment of the REMPI feature as a hot band: $9_0^1 19_1^1$. (As will be discussed in Section III.F, the D_9 vibration is in Fermi resonance in the S_1 state and so the notation for this assignment is simplistic.)

Exciting via the band at 734 cm^{-1} yields a ZEKE spectrum with the most intense band at 1436 cm^{-1}, being consistent with an assignment to 14^4, also present are the 14^2 band at 717 cm^{-1} and the 11^114^2 band at 1157 cm^{-1} – see Figure 3(d). This assignment is consistent with KK.[4] Unusually, in S_1, 14^2 is at 361 cm^{-1}, and so 14^4 being at 734 cm^{-1} is anomalous (also noted by KK)[4], suggesting a positive anharmonicity; this is plausible since the motion of D_{14} is ring puckering,[25] which would be pushing atoms closer together.

Exciting via the level at 753 cm^{-1} yields a ZEKE spectrum with the most intense band at 1339 cm^{-1}, which may be assigned 12^114^1, consistent with both KK[4] and the calculated values – see Figure 3(e) and Table 1. This then identifies a ZEKE band at 980 cm^{-1} as 12^1, with 14^1 also being seen, both consistent with the 12^114^1 assignment. Also seen in the spectrum are bands due to 14^2, 11^114^2 and 14^3. We also see the 11^114^2 band in the ZEKE spectrum obtained when exciting via the level at 770 cm^{-1} (unassigned by KK[4]) – see Figure 3(f) – and the wavenumber of this intermediate level is consistent with its being 11^114^2. There is thus some suggestion that the 753 cm^{-1} and 770 cm^{-1} S_1 levels arise from Fermi resonance between the 12^114^1 and 11^114^2 levels. KK[4] suggested that an LIF band at 789 cm^{-1} might be 11^114^2, but also that this may have arisen from the *p*DFB-Ar complex. This would not be at the expected wavenumber for 11^114^2 and further, we observed no ZEKE spectrum when exciting at this wavenumber; as a consequence, we reject that assignment.

F. Fermi resonance in the Region 800–830 cm^{-1}

1. ZEKE Spectra

This region of the REMPI spectrum contains a trio of bands that have been assigned by KK[4] to transitions involving totally-symmetric levels: 29^2, 9^1 and 11^2, with the last two having been assigned as a Fermi resonance in that work, in agreement with CP.[3] The three corresponding REMPI bands are at respective positions of 803 cm^{-1}, 819 cm^{-1} and 822 cm^{-1} – see Figure 4. In previous work[27,37,38,39]the 9^1 and 29^2 levels have been assigned as being in Fermi resonance in *p*FT, and this is also the case in *p*ClFB;[29,35] on the other hand, the 29^2 level in *p*Xyl, where it is more energetically removed from the 9^1 level, is at best exceptionally weak.[39] We have taken these observations to imply that the 29^2 transition is only active in the $S_1 \leftarrow S_0$ transition of these disubstituted benzenes by virtue of Fermi resonance, with its activity determined by how energetically proximate the 9^1 and 29^2 levels are.[39] In the present case of *p*DFB, the separation of these two levels is between that of *p*Xyl and *p*FT (and *p*ClFB) and as such, we might expect the appearance of 29^2 also to be attributable to Fermi resonance. We thus

recorded ZEKE spectra via these three intermediate levels, and these are presented in Figure 4(a)–(c), which also shows an expanded view of the relevant region of the REMPI spectrum. (Note that we have presented a preliminary discussion of these spectra[39] when comparing between four *para*-disubstituted benzenes.)

The ZEKE spectrum recorded via the band at 803 cm^{-1} is shown in Figure 4(a) and demonstrates the most intense band at 857 cm^{-1}, which can be straightforwardly assigned to 29^2. There are weak bands due to 28^1, 9^1 and $11^1 29^2$. The weak appearance of 9^1 is consistent with a Fermi resonance interaction: $9^1 \ldots 29^2$; note that we see no significant 11^2 band. Of interest is a band at 1035 cm^{-1}, whose assignment to the $17^1 19^1$ $\Delta v = 0$ band follows from the suggestion by KK[4] of the intermediate feature being the overlap of two bands; additionally, the $11^1 17^1 19^1$ band may be seen at 1475 cm^{-1}. This assignment yields values for the D_{17} vibration in the S_1 and D_0^+ states of 529 cm^{-1} and 730 cm^{-1}, respectively, which fit well with the calculated values (see Table 1). The derived S_1 value for D_{17} fits the calculated trends, namely that the experimental values lie below the calculated ones.

We now move on to considering the ZEKE spectra obtained when exciting via the bands at 819 and 822 cm^{-1} – see Figure 4(b) and (c). These bands were concluded to arise from a Fermi resonance pair, arising from a $11^2 \ldots 9^1$ interaction by CP[3] and this was agreed with by KK.[4] We now examine whether the ZEKE spectra confirm this. First, the spectrum obtained when exciting via the 822 cm^{-1} feature – Figure 4(c) – shows a progression in the D_{11} mode, with an intensity maximum for 11^3; this activity is in line with the most intense band in the ZEKE spectrum being for 11^2 when exciting via the 11^1 intermediate level – see Figure 2(e). The profile is unusual in that the 11^1 ZEKE band is more intense than might be expected from the profile inferred from the other members of the progression. We note that the 9^1 ZEKE band is somewhat weak in this spectrum, and there is also a weak band arising from 29^2. When we examine the 800–900 cm^{-1} region of the ZEKE spectrum obtained when exciting via the 819 cm^{-1} feature – Figure 4(b) – we see a very different picture: now the 9^1 band is locally the most intense, but with the 29^2 and 11^2 ZEKE bands being clearly seen. (The 29^2 band was seen in the two-colour MATI study,[10] with 29^2 being one of three possible assignments offered.) Of great prominence is the intensity of the 11^1 band, which is by far the most intense band in the spectrum; even if the intensities of the 0^0, 9^1 and 9^2 bands are summed, this would still be less than the intensity of the 11^1 band. This abnormally intense 11^1 band is also seen in the two-colour MATI study of Ref. 10, as well as in the REMPI-PES spectra of Sekreta et al.[6] and Bellm and Reid.[7] This unusual activity of the D_{11} vibration was also commented in the DF studies of CP[3] and KK,[4] and attributed to the Fermi resonance.

A weak ZEKE band at 462 cm^{-1} may be seen in Figure 4(c), and is marked with a ?, whose assignment is uncertain, but seems to be the 11^1 counterpart of the weak band at 22 cm^{-1} (also marked with a ?) that is seen close to the origin in the same spectrum; both of these bands were seen in the MATI study of Lembach and Brutschy,[10] where they were also unassigned.

In conclusion, we assign the three S_1 levels at 803 cm^{-1}, 819 cm^{-1} and 822 cm^{-1} respectively, to the following, where the leading term indicates the majority contribution and the … indicate Fermi resonance:

$29^2…9^1…11^2$

$9^1…29^2…11^2$

$11^2…9^1…29^2$

Interactions with the 29^2 level appear to be weak since the S_1 fundamental is at 401 cm^{-1}, and the overtone is close to the expected position, at 803 cm^{-1}, assuming small anharmonicity. This also seems to be the case for the 11^2 level, since the 11^1 band is at 411 cm^{-1} and the overtone is at 822 cm^{-1}. This picture is slightly complicated since the overtones may be expected to lie lower in wavenumber as the result of (diagonal) anharmonicity, and so their actual positions will be a combination of anharmonicity and Fermi resonance. Even so, in both cases the energetic shifts appear to be small.

2. Time-resolved photoelectron spectra

In Figure 5(a) we show two overlaid photoelectron spectra recorded using 1 ps laser pulses for pump and probe. These spectra were recorded with pump-probe time delays of 0 ps and 5 ps and clearly show the differing intensities of the photoelectron bands. In particular, the 0^0 band is strongest in the 0 ps spectrum and the 11^1 band is strongest in the spectrum recorded with a delay of 5 ps. The time-dependent intensity of the 0^0 band can be determined by scanning the delay stage; the result of this is plotted in Figure 6(a). (For time delays < 2 ps, the relative intensities are less reliable owing to strong field effects when the excitation and ionization laser beams are overlapped temporally.) A Fourier transform of the data in Figure 6(a) is shown in Figure 6(b), where two clear peaks may be seen at 3.6 cm^{-1} and 7.2 cm^{-1}; these features correspond to angular frequencies of 0.68 and 1.37 rad s^{-1}, and

oscillation periods of 9.2 and 4.6 ps, respectively. The peaks in the Fourier transform in Figure 6(b) correspond to the separation of the contributing vibrational eigenstates.

The angular frequencies from the Fourier transform were used as initial values in the following empirical equation for the time-dependence of the data in Figure 6(a):

$$C_a \cos(\omega_a t) + C_b \cos(\omega_b t) + C_c \qquad (1)$$

where the ω_i are the angular frequencies. Least-squares fitting to the time profile shown in Figure 6(a) very slightly refined values of the ω_i, giving wavenumber separations of the eigenstates as 3.6 cm^{-1} and 7.3 cm^{-1} and corresponding to periods of 9.2 ps and 4.6 ps, respectively. The fit to Equation 1 is robust – see Figure 6(a) – with R^2 = 0.96.

From the discussion of the ZEKE results above, and from the results of other work by CP[3] and KK,[4] we expect the 9^1 and 11^2 levels to be interacting. The deduced eigenstate spacing of 3.6 cm^{-1} is in excellent agreement with the REMPI spacing of 3.5 cm^{-1} between bands B and C in Figure 4, confirming this interaction. The other spacing of 7.2 cm^{-1} indicates the presence of a third state. The bandwidth (13 cm^{-1}) of the picosecond laser pulse was too narrow to encompass the 29^2… Fermi resonance component coherently with the other two eigenstates (see Figure 4), and so the 0 ps photoelectron spectrum in Figure 5(a) will not be completely indicative of the zero-order bright state, although it will contain a 29^2 contribution by virtue of its presence in the 9^1… and 11^2… eigenstates. The ~200 cm^{-1} resolution of the photoelectron spectrum was not sufficient to resolve the 9^1, 29^2 and 11^2 bands, which all lie under the third photoelectron band at ~850 cm^{-1} in Figure 5(a).

Looking at the possible totally symmetric levels that may be interacting, the only viable candidate for the third state is the $14^1 19^1 30^1$ level. However, this is expected to appear at a lower wavenumber in the S_1 state, and to result in a ZEKE band at 1033 cm^{-1}. No such band is observed and so this hypothesis is discarded. Because there are no other totally symmetric levels, we looked for levels of b_{3g} symmetry. A likely candidate is the $11^1 29^1$ level which could potentially couple via Coriolis coupling; however, this has a reduced likelihood under jet-cooled conditions, and so we suggest Herzberg-Teller coupling as the more likely possibility. This mechanism has previously been invoked in the S_1 state (see Section

IV.B.1), and is reminiscent of a related coupling seen in *p*FT between vibration-torsion (vibtor) levels.[40] There is a weak shoulder to the most intense REMPI band at ~820 cm^{-1}, which may be seen in the insert in Figure 1, and this matches the expected position for $11^1 29^1$. Furthermore, in the ZEKE spectra reported in Figure 4, which were recorded via the two most intense REMPI bands, we see a weak band at 870 cm^{-1}, which also fits the expected position of the $\Delta v = 0$ band for the $11^1 29^1$ transition. Hence, there is some evidence from the ZEKE spectra presented above to support the involvement of $11^1 29^1$ in the Fermi resonance in S_1. The evidence, such as the weak feature seen in the Fourier transform – Figure 6(b) – suggests that the interaction is weak.

In Figure 5(b) we show the time dependence of two of the cleanest contributions to the photoelectron spectra shown in Figure 5(a); these correspond to the 0^0 and 11^1 bands. These were determined by fitting the photoelectron peaks to Gaussian functions and then plotting the Gaussian areas as a function of time delay. The resulting intensity variations of the two bands are rather interesting. The behaviour of the 0^0 contribution is consistent with its being associated with the zero-order bright state, having maximum intensity at t = 0 ps. By contrast, the 11^1 band is out of phase, consistent with its being associated with a dark state, although its intensity does not drop to zero at any point. We interpret this in terms of there being non-zero FCFs between each of the 9^1 and 11^2 zero-order states and 11^1 in the cation, but it is also possible that the 11^2 zero-order state has a small amount of brightness, which would be consistent with other related molecules.[39] This unusual behaviour of the 11^1 band complicates the interpretation of the time-dependent behaviour and is consistent with suggestions from CP[3] and KK.[4] The inference from Figure 5(b) is that the majority contribution to the 11^1 photoelectron band comes from S_1 11^2, consistent with 9^1 being the zero-order bright state and 11^2 being the zero-order dark state. This picture is reminiscent of the behaviour seen for *p*FT when exciting via the 9^1 and 11^2 levels,[27] although in that case the 9^1 level is interacting with 29^2 in *p*FT, and 11^2 overlaps with $12^1 14^1$. With this in mind, we look back at the ZEKE spectra in Figure 4(b) and (c), which indicate that band B in the REMPI spectrum in Figure 4 is dominated by 9^1, while band C is dominated by 11^2. It is somewhat surprising that the 11^1 band is so intense in Figure 4(b), and in their fluorescence study KK[4] suggest that there are transition moment interference effects for these levels.

The third, highest wavenumber feature in Figure 5(a), required at least three Gaussian functions in order to model the photoelectron band profile at all times, consistent with the underlying $11^1 29^1$, 9^1, 11^2 and 29^2 bands discussed above. Because these overlap strongly it was not possible to perform a confident deconvolution of their time-dependence at this resolution.

G. ZEKE spectra recorded via bands in the range 880–960 cm^{-1}

An expanded view of this region of the REMPI spectrum is shown in Figure 7, and the ZEKE spectrum recorded via 0^0 + 880 cm^{-1} is shown in Figure 7(a). The intermediate level has been assigned[4] as $S_1\,18^2$, consistent with the strong Δv = 0 ZEKE band at 1023 cm^{-1}, allowing a value for D_{18} in the cation of 512 cm^{-1} to be established. The expected 11^118^2 and 9^118^2 bands may be seen to higher wavenumber, and the vibronically-induced 18^219^1 and 14^118^2 bands are also present. Although the 18^1 band appears to be too weak to observe, we do see the vibronically-induced 18^3 band.

There are three other REMPI bands in this region, at 935 cm^{-1}, 948 cm^{-1} and 954 cm^{-1}. The ZEKE spectra recorded via these levels form an interesting group, with a number of common bands that appear in all three spectra. Common bands (and their assignments) are: 991 cm^{-1} (20^230^2), 1260 cm^{-1} (15^119^1), and 1530 cm^{-1} (13^2). The strong ZEKE band at 991 cm^{-1} when exciting via 0^0 + 948 cm^{-1} and the strong 19^2, 11^119^2 and 11^219^2 bands when exciting via 0^0+954 cm^{-1} indicate that significant contributing levels to these two bands are 20^230^2 and 11^119^2, respectively, in agreement with the assignments by KK.[4] KK also suggested that 13^2 may be involved in these two levels and it appears to have its largest relative intensity when exciting at 0^0 + 954 cm^{-1}. Since the contributions from the 20^230^2, 15^119^1 and 13^2 levels appear across all three spectra, this supports the fact that they are all involved in a complex Fermi resonance. (A band assignable as 13^1 is seen when exciting at 0^0+948 and 0^0+954 cm^{-1}.)

On the other hand, a ZEKE band at 1286 cm^{-1} is seen only when exciting via 0^0 + 935 cm^{-1} suggesting that this may be an overlapped feature. Although the assignment of KK to 26^1 fits both their DF spectrum, and indeed the band in the ZEKE spectrum in Figure 7(b) according to the calculated cationic value (see Table 1), the S_1 calculated value is far removed from the excitation position, and so we are not happy with this assignment. We have no alternative assignment at the present time, and so leave the corresponding ZEKE feature unassigned – marked with a ? in Figure 7(b).

A weak ZEKE band is seen at 1011 cm^{-1} when exciting via the 954 cm^{-1} intermediate level, and this is a good fit to being a Δv = 0 band for 28^129^1, which is also be expected at this wavenumber.

In summary, we assign this trio of bands to the following, where the leading term of the Fermi resonance indicates the majority contribution:

935 cm^{-1}: $15^1 19^1 \ldots 13^2 \ldots 20^2 30^2$ + an unknown overlapped feature

948 cm^{-1}: $20^2 30^2 \ldots 13^2 \ldots 15^1 19^1$

954 cm^{-1} $13^2 \ldots 15^1 19^1 \ldots 20^2 30^2$ + overlapped $11^1 19^2$ and $28^1 29^1$

Thus, these are a rather complicated set of bands, and rather intriguing since the $20^2 30^2$, $15^1 19^1$ and 13^2 pervade the spectra, even though the 935 cm^{-1} band is more separated than the other two bands. In addition, two of the bands have extra contributions from overlapped features.

The assignment of these bands allows the values of the following vibrational wavenumbers to be deduced in the S_1 and D_0^+ states respectively, albeit acknowledging that there may be shifts from the Fermi resonance interactions: D_{13} as 477 cm^{-1} and 765 cm^{-1}; D_{15} as 660 cm^{-1} and 955 cm^{-1}; and D_{30} as 355 cm^{-1} (consistent with RS[2]) and 369 cm^{-1}.

H. Feature at 1059 cm^{-1}

An expanded view of this REMPI feature is shown in Figure 8, and it appears to have more than one contribution. KK[4] concluded there were two bands: at 1057 cm^{-1} (lower-wavenumber shoulder) and 1058 cm^{-1} (main band). They assigned the main band to $9^1 20^2$ and the shoulder to $16^1 18^1$ with possible contributions from 17^2 and $9^1 20^2$. We present two ZEKE spectra recorded via this feature, which are shown in Figure 8(a) and 8(b).

We consider first the ZEKE spectrum obtained via the dip in the more intense part of the band, which is shown in Figure 8(a). We can see that there are a number of strong ZEKE bands, and one of those at higher-wavenumber is consistent with being the 17^2 band at 1453 cm^{-1}, and we assign this as the Δv = 0 band, consistent with the D_{17} cation value derived in Section III. F. The band next to it at 1461 cm^{-1} may be assigned to $14^1 17^1 30^1$, which is totally symmetric. If we then consider the DF study by KK,[4] then we see that the expected S_0 position of this latter level is 1462 cm^{-1}, while for $16^1 18^1$ it would be 1343 cm^{-1}; thus, the unassigned 1470 cm^{-1} DF band seen by KK[4] nicely fits the $14^1 17^1 30^1$ assignment, and while the 1343 cm^{-1} DF band would be consistent with the $16^1 18^1$ assignment of KK, in the cation $16^1 18^1$ would be at 1357 cm^{-1}, and there is no clear ZEKE band at that position; of course, the activity in the two transitions might not necessarily be the same.

When exciting via the level dominated by 9^1 (Section III.F), unusual Franck-Condon factors were apparent, leading to the 11^1 band being the most intense, with also intensity in the 29^2 and 11^2 bands. We can see that this behaviour is consistent with a contribution from 9^120^2 to the ZEKE spectrum in Figure 8(a), with an intense band at 694 cm^{-1} (11^120^2) and the $\Delta v = 0$ band, 9^120^2 at 1089 cm^{-1} being much less intense; in addition, there is the close-lying 20^229^2 band, being of similar intensity. In contrast, the ZEKE spectrum in Figure 8(b) suggests that the 17^2 band dominates the eigenstate at 1060 cm^{-1}. Overall, these two spectra suggest that the low-wavenumber side of the REMPI band arises from 9^120^2, with perhaps some overlap/Fermi resonance with the main 17^2 band. The $14^117^130^1$ band is most prominent when exciting on the low wavenumber side of the feature. The Fermi resonance behaviour within this REMPI feature is a little unclear, particularly as there is an accidental resonance coincident with the 17^2 feature. It appears reasonable to assume that the $14^117^130^1$ activity results from Fermi resonance with 17^2, with the former feature appearing as a shoulder in Figure 8(b). The absence of the 11^120^2 and 9^120^2 bands in the latter spectrum suggests no Fermi resonance is occurring between 9^120^2 and 17^2.

This assignment to 9^120^2 would also lead us to expect to see a REMPI band arising from 11^120^2 (owing to the $29^2/9^1/11^2$ Fermi resonance); however, when we excite to slightly higher wavenumber, we only see a broadened feature around 1100 cm^{-1} in Figure 8(b), and no 11^120^2 band. (We also attempted to record ZEKE spectra on the far wings of the REMPI feature shown at the top of Figure 8, but we only saw clear features from accidental resonances in those cases.)

I. Bands in the range 1110–1140 cm^{-1}

There are three bands here, although KK[4] only mention one, at 1116 cm^{-1}, which they say consists of overlap/Fermi resonance with five features: 12^114^3, 14^6, 28^2, 18^220^2 and 7^1. When we excite via the 1114 cm^{-1} feature, we see a clean spectrum assignable to 7^1, with the 7^111^1 band also present – see Figure 8(c). When we excite at 1122 cm^{-1}, Figure 8(d), we see a spectrum that consists of two ZEKE bands: a band at 1168 cm^{-1}, which can be straightforwardly assigned to 28^2; and a band at 1275 cm^{-1} which may be assigned to 18^220^2, which fits both the S_1 and ZEKE band wavenumbers. Thus, this REMPI feature comprises two overlapped bands.

A weak REMPI band is also observed at 1130 cm^{-1} from which a very weak ZEKE spectrum was obtained. The ZEKE band positions were not consistent with the REMPI band being a cold feature, and indeed we assign this REMPI feature to a hot band corresponding to $9_0^1 11_0^1 19_1^1$.

J. Bands in the range 1150–1195 cm^{-1}

There are six REMPI bands in this region, an expanded version of which is shown at the top of Figure 9.

We were able to record a ZEKE spectrum when exciting at 0^0+1154 cm^{-1}, but the excitation wavenumber and the appearance of the spectrum confirmed that this REMPI band is a hot feature, assigned as $5_0^1 19_1^1$.

The ZEKE spectrum when exciting at 0^0+1165 cm^{-1} – Figure 9(a) – can straightforwardly be assigned as predominantly $11^1 12^1 14^1$, with the most intense bands being the Δv = -1 band at 1339 cm^{-1} and the Δv = 0 band at 1776 cm^{-1}. We also see clear $11^1 14^1$ and 12^1 component bands at 797 cm^{-1} and 980 cm^{-1}, and some other weak totally-symmetric bands (and associated vibronic bands). To higher wavenumber a band at 1957 cm^{-1} may be seen, and can be assigned to 12^2.

The ZEKE spectrum recorded via 0^0+1170 cm^{-1}, shown in Figure 9(b), may be seen to have a sizeable 12^2 band, suggesting this is the major contributor to the intermediate level, but there is still significant intensity from the bands associated with $11^1 12^1 14^1$. It is clear that the assignment of the 1165 cm^{-1} and 1170 cm^{-1} bands is to a Fermi resonance pair, $11^1 12^1 14^1 \ldots 12^2$ and $12^2 \ldots 11^1 12^1 14^1$, respectively. Interestingly, we also see the $14^2 29^2$ band at 1572 cm^{-1} in Figure 9(a), which will be commented further in the next paragraphs.

When we excite at 0^0 + 1179 cm^{-1} a very different ZEKE spectrum – Figure 9(c) – emerges that is dominated by the 1453 cm^{-1} band. Although this is very close to the wavenumber for the 17^2 band, that feature was a Δv = 0 band when exciting via the 1059 cm^{-1} feature (Section III.H); yet this does looks very much like a Δv = 0 band here. In addition, the expected S_0 value would be at 1380 cm^{-1} for 17^2, and there is no prominent band in the DF spectra when exciting via this feature;[4] and so we searched for an alternative assignment The only totally-symmetric combination band that appears to fit the S_1 excitation position and the ZEKE band wavenumber is $14^1 18^1 28^1$. This assignment would lead to an expectation of a DF band at ~1560 cm^{-1}, and indeed a band is seen at 1580 cm^{-1},[4] making this assignment, also suggested by KK, plausible. The band may be gaining intensity via interactions with the surrounding combinations that involve 14^2, as well as the $11^1 12^1 14^1$ transition.

We note that Reiser et al.[9] assigned the 1179 cm^{-1} intermediate to the 13^2 level in their ZEKE study, which was an uncertain assignment put forward by KK;[4] however, KK also suggested activity of the 13^2 when recording DF spectra from bands at ~950 cm^{-1} (see Section III.G). It would be unusual for Fermi resonance to occur over a range of > 100 cm^{-1}, and as we have commented above, the presence of 13^2 activity suggests involvement in a complex Fermi resonance involving two other levels in the 930–955 cm^{-1} region. Hence, we conclude that previous assignments of this feature[4,9] to 13^2 are incorrect.

There are other bands that are expected in this wavenumber region; in particular, the $9^1 14^2$, $14^2 29^2$ and $11^2 14^2$ bands, which correspond to combinations of 14^2 with each of the Fermi resonance triplet at 800–825 cm^{-1} and we now discuss the assignment of these.

We have already pointed out the presence of the $14^2 29^2$ ZEKE band when exciting at 1165 cm^{-1} – Figure 9(a). Exciting at 0^0+1184 cm^{-1} gives the ZEKE spectrum shown in Figure 9(d), with a band at 1596 cm^{-1} that can be assigned as $11^2 14^2$. There is also evidence of a small contribution from $9^1 14^2$ at 1558 cm^{-1}, which gives the expected more intense $11^1 14^2$ band at 1156 cm^{-1}. Thus, the source of these bands can be assigned as a level dominated by the S_1 $9^1 14^2$ level, with the intensities of the corresponding bands being similar to those for 9^1… – see Figure 4(b); this includes the $14^2 29^2$ band. There is also a weak $14^1 18^1 28^1$ band.

When exciting at 1187 cm^{-1} we assign the most intense band in the ZEKE spectrum in Figure 9(e) as $11^2 14^2$, which is the $\Delta v = 0$ band. Associated with this, cf. the 14^2 and 11^2… ZEKE spectra in Figures 2(c) and 4(c), we see the $14^2 19^1$, 14^3, $11^1 14^2$, $9^1 14^2$, $14^2 29^2$ and 14^4 bands. In addition, we see a sizeable $14^1 18^1 28^1$ band. The intermediate level is thus assigned as a level dominated by $11^2 14^2$.

The activity above suggests that the 1165 cm^{-1}, 1184 and 1187 cm^{-1} features comprise a complex Fermi resonance made up of bands corresponding to 14^2 in combination with the ($29^2/9^1/11^2$) Fermi resonance levels, with the overall activity being very similar to that seen in the spectra presented in Figure 4. This is complicated by contributions from the $14^1 18^1 28^1$ level to the 14^2 + ($29^2/9^1/11^2$) complex resonance, with a dominant contribution to the 1179 cm^{-1} band. In addition, overlapping this is a separate Fermi resonance involving the $11^1 12^1 14^1$ and 12^2 levels, with the lower one overlapping the Fermi resonance level dominated by $14^2 29^2$ – see top of Figure 9.

A very weak ZEKE spectrum was recorded via 0^0+1191 cm^{-1}, but its assignment is uncertain.

K. Bands in the range 1200–1250 cm^{-1}

In this region, in the absence of other interactions, we expect six bands arising from combinations of D_{29} and D_{11}, both with each of the members of the (29^2/9^1/11^1) Fermi resonance; an expanded version of this region of the REMPI spectrum is shown at the top of Figure 10. We recorded ZEKE spectra via each of these bands, with the ZEKE spectra displayed in Figure 10.

The weak band at 0^0+1208 cm^{-1} was not seen by KK[4]. It yields a weak ZEKE spectrum with a band at 1287 cm^{-1}, which provides a clear assignment to 29^3 – see Figure 10(a). This assigns the intermediate level to the 29^1 + [29^2…9^1…11^2] Fermi resonance component. The $11^1 29^3$ ZEKE band is present, but weak and overlapped with accidental resonance bands.

The band at 0^0 + 1217 cm^{-1} was also not seen by KK[4]. The ZEKE spectrum recorded via this feature is shown in Figure 10(b), ZEKE bands at 856 cm^{-1} and 1295 cm^{-1} may be seen, which are consistent with assignments to 29^2 and $11^1 29^2$, and hence the intermediate level contains $11^1 29^2$. It can be seen that the Δv = -1 band is the more intense, and weak bands due to 9^1 and 11^2 are also seen. The activity is consistent with the intermediate level being the 11^1 + (29^2…9^1…11^2) Fermi resonance component.

The ZEKE spectrum recorded at 0^0+1224 cm^{-1}, and shown in Figure 10(c), is straightforwardly assigned as arising from a $9^1 29^1$ contribution, with the expected dominance of $11^1 29^1$, and $9^1 29^1$ being the weaker Δv = 0 band – see Section III.F and Figure 4(b); the 29^3 band is also present; again, in line with expectations. We might expect to see contributions from $11^2 29^1$, but these are not obvious in this spectrum (the Δv = 0 band is expected at 1310 cm^{-1}). The assignment of this band to the Fermi resonance component 29^1 + (9^1…11^2…29^2) then follows. This assignment is consistent with that suggested by KK.[4]

The ZEKE spectrum shown in Figure 10(d) was recorded at 0^0+1227 cm^{-1}, and the S_1 level may be straightforwardly assigned as the Fermi resonance component 29^1 + (11^2…9^1…29^2), with the expected dominance of the $11^n 29^1$ progression.

The ZEKE spectrum recorded at 0^0+1232 cm^{-1}, and presented in Figure 10(e), has a clear assignment of 11^1 + (9^1…11^2…29^2), with all of the expected bands (noting again the stronger 11^2 and weaker $9^1 11^1$ bands).

Finally, the ZEKE spectrum recorded via at 0^0+1236 cm^{-1} is given in Figure 10(f), and yields an assignment of the S_1 level to 11^1 + (11^2…9^1…29^2).

KK[4] only assigned one of the previous two bands to $9^1 11^1$, which was likely our 1232 cm^{-1} band as it is the more intense.

Thus, these six REMPI bands seem to be straightforwardly assignable as the expected six combinations. These fall into two distinct groups with the 29^1 combinations being of b_{3g} symmetry, while the 11^1 combinations are of a_g symmetry. It is thus unsurprising, given the absence of any other nearby bands, that the spacings between each set of combinations are essentially the same, and concur with those of the parent $29^2/9^1/11^2$ Fermi resonance triplet.

KK[4] suggested that the 1236 cm^{-1} feature may contain contributions from 16^2 and $14^2 18^2$; however, both of these would lie outside of the region we scanned, and that the former transition is thought to be associated with the REMPI band at 1252 cm^{-1} (see Section III.L and Table 1). Thus, these possible additional contributions are still uncertain, but seem unlikely.

L. Bands in the range 1250–1340 cm^{-1}

An expanded version of this region of the REMPI spectrum is shown at the top of Figure 11. The ZEKE spectrum recorded via 0^0+1252 cm^{-1}, Figure 11(a), shows a strong $\Delta v = 0$ band at 1689 cm^{-1}, whose assignment was initially unclear. The appearance of a ZEKE band at 1378 cm^{-1}, which can be assigned as 5^1, suggests that the 1689 cm^{-1} band comes from a totally symmetric vibration. There are not many possible assignments that are consistent with a $\Delta v = 0$ shift between the S_1 and D_0^+ states of ~440 cm^{-1} except for 16^2; this would yield a cation value of 845 cm^{-1} and an S_1 value of 626 cm^{-1}. While the latter is close to the 619 cm^{-1} assignment from KK,[4] this came from the assignment of a $16^1 18^1$ band via the 1059 cm^{-1} feature, but we did not see the corresponding ZEKE band (see Section III.H), casting doubt on that assignment, and so we favour an assignment of 16^2 for the 1252 cm^{-1} REMPI band.

The ZEKE spectrum obtained when exciting via 0^0+1256 cm^{-1}, Figure 11(b), yields a strong $\Delta v = 0$ band at 1377 cm^{-1}, allowing an assignment to 5^1, which concurs with KK.[4] Other bands are straightforwardly assigned to totally-symmetric vibrations, with the small band at 1689 cm^{-1} suggesting a weak 5^1…16^2 Fermi resonance. Interestingly, we see the 19^1 vibronically-induced band, but not 14^1. Although time-

resolved photoelectron spectra were recorded via the coherent excitation of the 1252 and 1256 cm^{-1} bands in the present work, no time dependence was observed, suggesting that any coupling with 16^2 is weak.

The ZEKE spectrum obtained when exciting via 0^0+1290 cm^{-1}, Figure 11(c), yields two strong bands that can be assigned as 11^118^2 and 11^218^2, with the S_1 excitation position allowing an assignment to the intermediate as 11^118^2 in agreement with KK.[4] We also see the totally symmetric bands 18^2 and 9^118^2.

IV. FURTHER DISCUSSION

A. Fermi Resonances

The Fermi resonance between the 9^1 and 11^2 levels has been discussed by CP[3] and KK[4]. As may be seen from the expanded view of this region of the REMPI spectrum at the top of Figure 4, bands B and C are very close together, with a third, band A, to lower wavenumber. CP[3] scanned across the region corresponding to bands B and C recording DF spectra. They found that the 11_2 activity was dominant when exciting to higher wavenumber, while 9_1 was more active to lower wavenumber (which is in-line with our ZEKE spectra). This, and the presence of bands associated with both transitions in all spectra, led them to the conclusion that bands B and C (in the REMPI spectrum of Figure 4) comprised a Fermi resonance. This conclusion was also supported by KK,[4] and both papers also provided some explanation of the surprisingly intense 11_1 band in the DF spectra.

In the present work – see Section III.F – we concur with the above, but we also conclude that the S_1 29^2 band is part of the Fermi resonance, consistent with the Fermi resonance between 9^1 and 29^2 seen in *p*FT,[27,39] where these two levels are very close together. The ZEKE spectra suggest that both the $9^1…29^2$ and $9^1…11^2$ interactions are significant, while the $29^2…11^2$ interaction is weak. The latter may be viewed as a Darling-Dennison interaction, but interestingly the interaction is not direct, but appears only to occur by virtue of the pairwise interactions with 9^1.

As noted above, we also studied this Fermi resonance using time-resolved photoelectron spectroscopy using picosecond laser pulses. This work confirmed that the main interaction was between the 9^1 and 11^2 levels, but implied a weak interaction with the 11^129^1 level, probably by

Herzberg-Teller coupling. Since we do not see any evidence of such coupling between 11^1 and 29^1 – see Section III.D and Figure 2 – then the interaction must be directly with the 9^1 zero-order bright state.

We now comment on a time-resolved study by Long et al.[41] In that work, a 45 fs UV pulse (266.7 nm) was used to excite the $S_1 \leftarrow S_0$ transition and then after a delay of tens of picoseconds, multiple photons from a second pulse (~800 nm) ionized the molecule; photoelectron spectra were then recorded and their variation with time delay was used as a probe of the dynamical processes occurring in the S_1 state. The pulse width corresponds to ~490 cm^{-1} meaning that vibrational selectivity is limited. In that work,[41] it was concluded that it was likely that the 11^1 and 9^1 modes were excited, and since they were referring to the work by CP[3] and KK[4], the 9^1 transition was noted as being the $9^1 \ldots 11^2$ Fermi resonance (while we conclude here that there is involvement from 29^2 also). Owing to this poor energy resolution, it was difficult to interpret the photoelectron spectrum presented in Ref. 41, which was thought to consist of contributions from both exciting via 11^1 and the $9^1 \ldots 11^2$ Fermi resonance (although it seems that the former transition would only just be caught by the wings of the laser pulse); additionally, the resolution of the photoelectron spectrum seems to be > 700 cm^{-1}. Further, the two photoelectron bands that resulted from ionization from the Fermi resonance levels appear to correspond to levels of the ion that lie far above the AIE. These aspects led the authors to conclude that the assignment of the intermediate level was far from clear, but they did see oscillations of photoelectron band intensities that had a period consistent with the separation of the 9^1 and 11^2 levels.

The three bands in the 930–960 cm^{-1} range, see Section III.G, also arise from a three-way Fermi resonance between 15^119^1, 13^2 and 20^230^2. All three $\Delta v = 0$ features appear in each of the ZEKE spectra exciting via each of these bands, and the relative intensities suggest that all three eigenstates are quite mixed. As we indicated above, there is an unidentified ZEKE band at 1286 cm^{-1} that appears to arise from an S_1 level that does not form part of the interactions. In addition, the 954 cm^{-1} feature contains a clear overlapped transition with 11^119^2, together with the weak 28^129^1. On the basis of quantum number changes, ΔN, in particular that small differences in vibrational quantum number between coupled levels are favoured,[42] it may have been expected that the 11^119^2 and 15^119^1 bands would interact strongly, but this does not seem to be the case. By the same argument, it is surprising that there is apparently strong mixing between the 15^119^1, 13^2 and 20^230^2 levels, where $\Delta N = 4$ or 6.

The 1059 cm^{-1} feature, see Section III.H, was found to comprise a $17^2\ldots14^1 17^1 30^1$ Fermi resonance, as well as an overlapping $9^1 20^2$ contribution. Interestingly, the $9^1 20^2$ band seems cleanest on the low-wavenumber side of the band, but there is not the switch in intensity to the $11^2 20^2$ band (at 1140 cm^{-1}), which the underlying $29^2/9^1/11^2$ Fermi resonance would suggest, although there is significant broadening. Finally, we see no clear evidence for the $16^1 18^1$ band in the ZEKE spectrum, which was suggested as being present by KK,[4] and although we cannot conclusively rule out the possibility that its contribution is narrow in wavenumber and that we missed this, it seems unlikely.

The bands that occur in the 1160–1195 cm^{-1} region – see top of Figure 9 – are very interesting in that they are made up of two overlapping Fermi resonances of the same symmetry (see Section III.J) yet they appear to be almost completely distinct. The first of these comprises four levels that are made up of the 14^2 in combination with each of the three $29^2/9^1/11^2$ Fermi resonance levels, and also $14^1 18^1 28^1$. These are then overlapped with a two-component Fermi resonance, $11^1 12^1 14^1\ldots12^2$. The ZEKE spectra clearly indicate the contributing eigenstates, allowing this complicated picture to be unravelled.

We have also unpicked the assignments of the bands in the range 1205–1240 cm^{-1} – see top of Figure 10 and Section III.K – which are found to comprise six bands, made up of two distinct complex Fermi resonances: 29^1 in combination with each of the $29^2/9^1/11^2$ Fermi resonance components; and corresponding component bands between 11^1 and $29^2/9^1/11^2$. These two sets of three levels have b_{3g} and a_g symmetry, respectively, and hence are not expected to interact directly; this is borne out by the ZEKE spectra.

As well as the $9^1\ldots11^2$ Fermi resonance discussed in the KK[4] paper, aspects of the other abovementioned Fermi resonances are commented on in the supplementary information of that work, as noted in the above text, although not all of the bands discussed in the present work were seen.

B. Vibronic coupling

1. $S_1 \leftarrow S_0$ transition

The S_1 $^1B_{2u} \leftarrow S_0$ $^1A_{1g}$ transition in benzene is a classic case of Herzberg-Teller coupling, where the transition is electric-dipole forbidden, but becomes allowed via vibronic interactions that may be viewed as intensity stealing of the S_1 state from a higher electric-dipole allowed $^1E_{1u}$ state. The vibronic interaction induces activity in vibrations of e_{2g} symmetry in the S_1 state. Benzene has the outermost π electronic configuration $\ldots a_{2u}^2 e_{1g}^2 e_{2u}^0 b_{2g}^0$. The degeneracies of the *e* orbitals are lost in D_{2h}, and this π electronic configuration becomes: $\ldots b_{3u}^2 b_{1g}^2 b_{2g}^2 a_u^0 b_{3u}^0 b_{2g}^0$ for *p*DFB, although other low-lying unoccupied orbitals may be present. Although the $S_1 \leftarrow S_0$ transition, corresponding to an $a_u \leftarrow b_{2g}$ excitation, becomes allowed under D_{2h} point group symmetry, vibronic coupling can still occur and this leads to activity in b_{3g} modes; in particular, the D_{29} vibration appears to be the most active and the 29^1 band is seen clearly in the REMPI spectrum in Figure 1, with the 28^1 transition also being seen but weaker. Although transitions involving a_g vibrations are Franck-Condon allowed, in principle the intensities of these can be affected by vibronic coupling.[36] The observation of non-Franck-Condon active modes opens up the ability to obtain information on the corresponding vibrations of the cation.

KK[4] commented on the possible role of other coupling mechanisms in the S_1 state, partly justified by: the observation of combination bands of overall a_g symmetry, but involving non-totally-symmetric modes (such as $12^1 14^1$); the large change in wavenumber of some vibrations between the S_0 and S_1 states; and the change in vibrational activity between one-photon and two-photon electronic spectra. In principle, combination bands can occur as the result of anharmonic (Fermi resonance) coupling and the large changes in wavenumber appear to be the result of electronic structure changes (e.g. the calculated wavenumber of the D_{14} mode of (mono)fluorobenzene is much higher in the S_1 state than the S_0 state in the absence of any vibronic coupling[43], and is in good agreement with the experimental value). The difference in one- and two-photon electronic spectra has also been discussed by Blease et al.[36] and also attributed to vibronic coupling.

2. $D_0^+ \leftarrow S_1$ transition

In the low-wavenumber region of the ZEKE spectrum obtained when exciting via the S_1 origin, as well as a number of S_1 totally-symmetric modes, we observe three main Franck-Condon-forbidden bands, D_{20}, D_{19} and D_{14}, which have respective symmetries b_{3u}, b_{2g} and a_u.

If we consider the ionization involving the vibronic levels of the S_1 and D_0^+ states, ignoring the departing electron, then the transition moment will be given by:

$$< \psi'_{ev}|\mu|\psi^+_{ev} >$$

(2)

Taking into account the electronic symmetries of the S_1 and D_0^+ states, as well as the symmetries of the three components of μ, then the symmetry condition for a vibronically-allowed transition may be derived to be:

$$\Gamma(\psi_v')\times\Gamma(\psi_v^+) \supseteq b_{1g}, b_{2g}, b_{3g}$$

(3)

but this would only be consistent with ionization to the 19^1 level becoming allowed, when exciting from an S_1 totally-symmetric vibrational level, such as the zero-point level. Even then, the vibronic transition would have to steal intensity from an excited ($B_{2g}\times b_{2g}=$) A_g cationic state via a Herzberg-Teller mechanism, and no such state exists low enough in energy[15] for this to be viable.

We now consider the case where we view the ZEKE process as an excitation to a high-lying Rydberg state. First of all, we note that the symmetries of a Rydberg electron in D_{2h} symmetry are:[9]

s: a_g (sσ)

p: b_{1u} (pσ); b_{2u}+b_{3u} (pπ)

d: a_g (pσ); a_g + b_{1g} (dπ); b_{2g}+b_{3g}(dδ)

f: b_{1u} (fσ); b_{2u}+b_{3u} (fπ); a_u + b_{1u} (fδ); b_{2u}+b_{3u} (fϕ)

As such, and as stated in Ref. 9, these cover all of the D_{2h} symmetry classes, and so in principle it is possible to combine the symmetry of the cation wavefunction with that of an appropriate Rydberg electron to yield a Rydberg state of the correct symmetry to undergo Herzberg-Teller intensity stealing from any low-lying excited state. The lowest-lying cationic state is of B_{1g} symmetry at ~ 1 eV, with other states at lying > 2.7 eV.[15] So if we assume it is Herzberg-Teller coupling between Rydberg states that have $^2B_{2g}$ (i.e. D_0^+) and $^2B_{1g}$ cationic cores that causes the observation of the three Franck-Condon-forbidden vibrations, D_{20}, D_{19} and D_{14}, then we can deduce an appropriate choice of Rydberg electron in each of these would lead to an allowed transition, and then can consider whether this is a viable Herzberg-Teller interaction involving the B_{1g} cation state – or rather the Rydberg states thereof.

The allowed symmetries of the Rydberg electron, $\Gamma(\psi_{Ryd})$ that may be excited from the S_1 state can be deduced from:

$$\Gamma(\psi_{Ryd}) = \Gamma(\psi_e,S_1)\times\Gamma(\psi_{vib},S_1)\times\Gamma(\mu)\times\Gamma(\psi_e,D_0^+)\times\Gamma(\psi_{vib},D_0^+) \quad (4)$$

which simplifies to:

$$\Gamma(\psi_{Ryd}) = (b_{1g},b_{2g},b_{3g}) \times \Gamma(\psi_{vib},D_0^+) \quad (5)$$

Hence, for activity in the D_{19} vibration when exciting from the S_1 vibrationless level, we would require $\Gamma(\psi_{Ryd}) = (b_{3g}, a_g, b_{1g})$, with the corresponding symmetries for D_{20} and D_{14} being (b_{2u}, b_{1u}, a_u) and (b_{1u}, b_{2u}, b_{3u}).

It seems reasonable to assume that if the electronic symmetry of the Rydberg state is pertinent, and is obtained from the combination of the cation core and the Rydberg electron, then the Rydberg electron and the electrons of the cationic core should interact. This suggests that the coupling will be strongest if the Rydberg electron is s or p, in both Rydberg states, which are the most penetrating. (Although subsequent l and m_l mixing may occur,[44] this will be subsequent to the transition to the Rydberg state.) So, for the D_{19} mode, this would require the Rydberg electron to be s, and so the Rydberg vibronic symmetry to be $B_{2g}\times b_{2g}\times a_g = A_g$. As already noted, the lowest cationic excited state is of B_{1g} symmetry,[15] and so when combined with Rydberg symmetries for s and p electrons, this yields Rydberg state symmetries of B_{1g}, A_u, B_{3u} and B_{2u}, none of which are of the correct symmetry to interact with the D_0^+ 19^1 vibronic level. As such, the Herzberg-Teller mechanism does not appear to be viable for 19^1. In a similar way, D_{20} would require a p electron, and to have Rydberg vibronic symmetries of $B_{2g}\times b_{3u}\times b_{1u} = A_g$ or $B_{2g}\times b_{3u}\times b_{2u} = B_{3g}$, with neither of these being able to couple to the Rydberg states of lowest-lying excited cation state. Finally, in a similar way, D_{14} would require a p electron, and have Rydberg vibronic symmetries of $B_{2g}\times a_u\times b_{1u} = B_{3g}$, $B_{2g}\times a_u\times b_{2u} = A_g$, or $B_{2g}\times a_u\times b_{3u} = B_{1g}$, with only the latter one being viable. Hence, although vibronic coupling is a possible explanation for the activity of 14^1, it is not viable for 19^1 or 20^1.

At this point, we also note that the same Franck-Condon-forbidden vibrations appear in the low wavenumber region of the one-colour MATI spectrum of Kwon et al.,[11] with what appear to be similar intensities. Since the ionization there occurs from the S_0 state, which has A_g symmetry, then this modifies the symmetry arguments. For example, excitation to p Rydberg states is possible for 19^1, giving the Rydberg vibronic symmetries as $B_{2g}\times b_{2g}\times b_{1u} = B_{1u}$, $B_{2g}\times b_{2g}\times b_{2u} = B_{2u}$ or $B_{2g}\times b_{2g}\times b_{3u} = B_{3u}$, with two of these allowing Herzberg Teller interaction with the Rydberg states arising from the B_{1g} excited cationic core and a p Rydberg electron. However, 20^1 would require an s electron, and so a Rydberg vibronic symmetry of $B_{2g}\times b_{3u}\times a_g = B_{1u}$, which cannot interact with the lowest excited Rydberg states. In a similar way, 14^1 requires an s electron, and a Rydberg vibronic symmetry of $B_{2g}\times a_u\times a_g = B_{2u}$ –which can interact with the excited Rydberg states. Hence, although vibronic coupling is now a possible explanation for the activity of 14^1 and 19^1, it does not appear to be viable for 20^1.

Herzberg-Teller coupling is an intensity stealing mechanism resulting from vibronic interactions between electronic states, and is termed interchannel coupling. Poliakoff, Lucchese and coworkers have recently been developing the idea of intrachannel coupling,[45] initially as an explanation for the activity of Franck-Condon-forbidden π bending vibrations in the photoelectron spectra of CO_2.[46] This work has now been expanded to other molecules, and some attention has been given to polyatomic molecules,[47] and applied by others to chiral molecules.[48] The theory does not depend on the Herzberg-Teller intensity stealing mechanism, but does depend on the non-separability of the electronic and nuclear motion, in requiring the transition moment for ionization to be dependent on the vibrational motion. The mechanism effectively involves the departing electron interacting with the potential of the core, which has a vibrational dependence; as such, the symmetry of the departing electron is brought into the argument, but does not require any intensity stealing to be invoked.[45,47] In the present work we have extended these arguments to include the formation of high-lying Rydberg states that are populated in ZEKE experiments. Of note is that the three non-Franck-Condon-active modes, D_{20}, D_{19} and D_{14} have the lowest wavenumber of all of the modes of *p*DFB and so may reasonably be expected to have the largest nuclear displacement during their vibrations.

In summary, we hypothesise that the intrachannel coupling mechanism applies to the ZEKE Rydberg states prior to any l and m_l mixing and field ionization, and that s and p Rydberg electrons are expected to couple more strongly with the D_0^+ core. We then assume the Rydberg states must satisfy both the symmetry requirements for the excitation step from the intermediate level, and those for intrachannel vibronic coupling. The important point is that the position and symmetry of higher cationic states are now irrelevant. This would explain the similar non-Franck-Condon activity for both the two-colour ZEKE and the one-colour MATI spectra referred to above. Also, in the conventional photoelectron spectrum in Figure 5(a), there do appear to be contributions from non-Franck-Condon vibrations between the 0^0 and 11^1 bands, although it is not possible to say whether all three vibrations are active.

From Table 1 it can be seen that D_{30} has a wavenumber similar to that of D_{14} in the cation, and so it may be wondered why this is not active. We note that D_{30} is an in-plane vibration (see Table 1 and Ref. 25), and the ionization is occurring from a π or π* orbital in the case of the S_0 and S_1 states, respectively. As such, it seems more likely that out-of-plane vibrations will interact with the outgoing electron, and so become active.

3. Vibrational wavenumbers

The vibrational wavenumbers of the S_0 state have been discussed in detail in Ref. 25. We also made some comments on the vibrational wavenumbers of the S_1 state of *p*DFB in Ref. 27 in relation to those of *p*FT. To that discussion we add here that we believe we have strong evidence for the 7^1 transition at 1114 cm^{-1} and so can confirm the provisional assignment given by KK.[4] In addition, we confirm many other S_1 wavenumbers. For all S_1 vibrational wavenumbers that have been determined or confirmed in our work, the agreement between the calculated and experimental values is good, except for D_{14}, which we have pointed out in earlier work[26,27,35] is poorly described by DFT methods. The agreement is fair for two other experimentally-determined values (see Table 1), D_{10} and D_{27}, which were not confirmed in the present work. On the other hand the agreement for one a_g, two b_{3g} and one b_{2u} modes is exceptionally poor: D_4, D_{23}, D_{25} and D_{26}. The first three of these come from the two-photon study of RS[2], while the last was put forward by KK.[4] We have discussed the 1286 cm^{-1} ZEKE band observed via the 933 cm^{-1} intermediate S_1 level in Section III.G. Although we have an assignment for the 933 cm^{-1} feature, we presently assume there is an unidentified overlapping feature here that gives rise to the (also unidentified) 1286 cm^{-1} band (although either $9^1 11^1$ or 29^3 are possible assignments for this band, neither is expected with this intensity via this feature). Currently, therefore, the assignment of the D_4, D_{23}, D_{25} and D_{26} vibrations must remain tentative.

We now move onto the cation. As with the S_0 state, we expect the calculated wavenumbers to be in good agreement with the experimentally-derived values, and this is true for all of the values derived from the ZEKE spectra, many of which are consistent with those from the other ZEKE or MATI studies. In the one-photon MATI spectrum of Ref. 11, values for most of the cation vibrations were given, but assignments could only be based upon the calculated wavenumbers, combined with expectations that totally-symmetric vibrations were the most active. That said, a number of the assignments were uncertain and we feel that the assignments of a number of the non-totally-symmetric vibrations are incorrect. For example, the values assigned in Ref. 11 to vibrations D_{22}–D_{27} (see Table 1) could be assigned, respectively, to the totally symmetric modes $5^1 9^2$, 17^2, $9^1 11^1 20^2$, $16^1 18^1$ or $19^2 30^2$, $9^1 11^1$ and $20^2 29^2$. Additionally, values of 743/731 cm^{-1} that were suggested as being assignable to D_{10} or D_{17} could be assigned to 30^2 and 14^2, while the 1015 cm^{-1} value given for D_{12} or D_{15} is possibly $28^1 29^1$. Also, given the comments in Section IV.B. and the results of the present work, the band observed with a wavenumber of 368 cm^{-1} that was suggested in Ref. 11 as being either D_{14} or D_{30} is likely the former. These reassignments are much more in line with the expected symmetries of active vibrations, even taking into account vibronic coupling.

Finally, we also pointed out in Section III.J that the previous value of 726 cm^{-1} assigned to D_{13} in the cation[9] was incorrect, and similarly that the value of 859 cm^{-1} ascribed to D_{16} in Ref. 11 and taken from Ref. 10 is an incorrect assignment, with the authors of Ref. 10 suggesting three possible assignments; one of these was 29^2, which is the assignment we are confident of from the present ZEKE results.

V. CONCLUDING REMARKS

In this work we have presented ZEKE spectra recorded via all significant S_1 levels that are active in the 0–1300 cm^{-1} region of the one-photon $S_1 \leftarrow S_0$ transition. In so doing, we have been able to confirm the assignments of almost all bands discussed by Knight and Kable,[4] but have clarified some of these while uncovering a number of complex Fermi resonances, some of which are associated with bands not explicitly mentioned in Ref. 4. This has also allowed the confident confirmation or establishment of the wavenumbers of seventeen vibrations in the D_0^+ state. Many of these vibrations have been identified as $\Delta v = 0$ bands in ZEKE spectra, and are seen across a number of spectra, giving weight to their assignments; that the results are also in good agreement with the calculated values gives additional credence to these.

Statistical (or dissipative) IVR is expected to occur at > 2000 cm^{-1} in *p*DFB.[4] In the present work we have seen examples of the sporadic build-up of vibrational coupling via the identification of a number of complex Fermi resonances at < 1300 cm^{-1}. This sporadic nature of the build-up of the density of states was highlighted in recent work.[39] It is also interesting that, although there was the expected non-interaction between overlapping Fermi resonance features of different symmetry, there were cases of components of the same symmetry overlapping but not interacting (see Section III.J), suggesting the coupling of zero-order states also depends on the relative motions of the vibrations, as well as their symmetry.

We have also considered the appearance of non-Franck-Condon-allowed vibrations in the low-wavenumber region of the ZEKE spectrum recorded via the S_1 origin. We extended the arguments of Ref. 45 to include high-lying Rydberg states, and suggest that *n*s and *n*p Rydberg states are more likely to be involved in intrachannel coupling. We have also suggested that for ionization from π or π* orbitals in substituted benzenes, it is more likely that out-of-plane vibrations are more likely to lead to such interactions.

Acknowledgements

We are grateful to the EPSRC for funding (grants EP/L021366/1 and EP/E046150). The EPSRC and the University of Nottingham are thanked for studentships to W.D.T., D.J.K and J.M. The High Performance Computer resource at the University of Nottingham was employed for the quantum chemistry calculations.

Table I: Calculated and experimental vibrational wavenumbers (cm^{-1}) for the S_0, S_1 and D_0^+ electronic states of *p*DFB

D_i[a]	Mulliken (D_{2h})[b]	Wilson/Varsányi labels[c]	Duschinsky[d]	S_0		S_1			D_0^+				
				Expt[e]	Calc.[f]	Expt[g]	Expt (This work)	Calc.[h]	Expt[i]	Expt[j]	Expt[k]	Expt (This work)	Calc.[l]
D_1	1(a_g)	2	**2**,7a	3088	3114			3143	3098		3015		3118
D_2	10(b_{1u})	20a	**13**,20a	3073	3100			3131			3094		3108
D_3	2(a_g)	8a	**9a**	1615	1595			1519	1640	1600	1640	1642	1628
D_4	11(b_{1u})	19a	**18a**,(20a)	1514	1492	1335		1422					1457
D_5	3(a_g)	7a	1,7a,(2,6a)	1257	1226	1251	1256	1235	1375	1340	1379	1377	1350
D_6	12(b_{1u})	13	12,19a,20a,(13 18a)	1228	1187	1015		1198					1274
D_7	4(a_g)	9a	**8a**	1140	1126	[1116][m]	1114	1099	1148	1110	1152	1152	1137
D_8	13(b_{1u})	18a	**19a**,12	1014	999	937		951			983		956
D_9	5(a_g)	1	1,6a,(7a,2)	859	841	818	818	820	836	830	839	839	823
D_{10}	14(b_{1u})	12	20a,12,(19a,13)	740	724	[666][m]		710			743/731[n]		726
D_{11}	6(a_g)	6a	**6a**,7a,(2,1)	450	443	410	411	414	439	430	441	441	435
D_{12}	7(a_u)	17a	**17a**	945	939	583	585	501			1015[o]	980	972
D_{13}	9(b_{1g})	10a	**10a**	800	792	475[p]	477	429	726[q]		768	765	760
D_{14}	8(a_u)	16a	**16a**	422	424	175	168	97[r]	359	350	368[s]	361	360
D_{15}	15(b_{2g})	5	**5**,10b	928	927	670	660	697			1015[o]	955	978
D_{16}	28(b_{3u})	11	**17b**,11,(16b)	838	835	619	626	667	859			845	864
D_{17}	16(b_{2g})	4	**4**,(10b)	692	694	528	529	567			743/731[n]	730	710
D_{18}	29(b_{3u})	16b	**16b**,11,(17b)	505	505	438	440	487	508	510	515	512	506
D_{19}	17(b_{2g})	10b	**10b**,4,(5)	374	363	274	273	279	303		303	305	289
D_{20}	30(b_{3u})	17b	16b,17b,11	158	154	120	120	124	127	130	124	127	123
D_{21}	18(b_{2u})	20b	**20b**	3091	3113			3139					3117
D_{22}	23(b_{3g})	7b	**7b**	3085	3102			3126			3054		3109
D_{23}	24(b_{3g})	8b	**9b**	1617	1601	1516		1407			1459		1388
D_{24}	19(b_{2u})	19b	**18b**,(19b,14,15)	1437	1400			1397			1526		1472
D_{25}	20(b_{2u})	14	**15**,(14)	1306	1287	1591		1317			1351		1311
D_{26}	25(b_{3g})	9b	**3**,8b	1285	1268	[933][m]		1232			1278		1238
D_{27}	21(b_{2u})	15	**14**,19b	1085	1074	1100		1022			1113		1096
D_{28}	26(b_{3g})	6b	**6b**,(8b)	635	628	558	558	553			583	584	572
D_{29}	27(b_{3g})	3	8b,6b,(3)	446	435	403	401	396	430			429	424
D_{30}	22(b_{2u})	18b	19b,14,18b	348	337	352	355	347			368[s]	369	357

a) See Ref. 25 for the form of these vibrations and further discussion.

b) Mulliken[30]/Herzberg[31] numbering.

c) Given as Wilson labels in Ref. 4 without any detailed comment.

d) Normal modes of *p*DFB expressed in terms of those of benzene using a generalized Duschinsky approach – see Ref. 25.

e) Evaluated set of values discussed in Ref. 25.

f) B3LYP/aug-cc-pVTZ scaled by 0.97.[25]

g) LIF values from Ref. 4.

h) TD-B3LYP/aug-cc-pVTZ scaled by 0.97.[27]

i) Two-colour ZEKE spectroscopy.[9]

j) Two-colour REMPI-PES spectroscopy.[6]

k) One-colour MATI spectroscopy.[11]

l) UB3LYP/aug-cc-pVTZ scaled by 0.97.[27] These results are in excellent agreement with the B3LYP/6-311++G(2df,2pd) values of Ref. 11 (we assumed these were unrestricted also), particularly if those values are scaled by 0.97 also.

m) These assignments were not supported by DF spectra in Ref. 4.

n) In Ref. 11, it was not possible to decide between the assignment of one or other of these values to D_{10} or D_{17}.

o) In Ref. 11, it was not possible to decide between the assignment of this value to D_{12} or D_{15}.

p) In Ref. 4, two possible assignments for D_{13} were put forward: 588 cm^{-1} and 475 cm^{-1}. As we noted in Ref. 27, the lower value is in better agreement with the calculated value, and herein we have seen that the ZEKE spectra also support this lower value – see text.

q) We believe this assignment to be incorrect – see text.

r) The calculated value for D_{14} in the S_1 state using TD-B3LYP is highly unreliable – see Refs. 26, 27 and 35.

s) In Ref. 11, it was not possible to decide between the assignment of this value to D_{14} or D_{30}.

Figure Captions

Figure 1: Two-colour (1+1′) REMPI spectrum of the 0–1300 cm^{-1} region of the *p*DFB $S_1 \leftarrow S_0$ transition. Hot band positions are identified with a red dot. The assignments are discussed in the text.

Figure 2: ZEKE spectra recorded via the indicated S_1 resonances. The indicated intermediate level is assigned as the major contributor – see text for discussion of the assignments. Asterisks and obeli (†) indicate accidental resonances and are discussed in Section III.B.

Figure 3: ZEKE spectra recorded via the indicated S_1 resonances. The indicated intermediate level is assigned as the major contributor – see text for discussion of the assignments. Asterisks and obeli (†) indicate accidental resonances and are discussed in Section III.B.

Figure 4: ZEKE spectra via the S_1 $29^2/9^1/11^2$ Fermi resonance. An expanded view of the 780–860 cm^{-1} region of the REMPI spectrum shown in Figure 1 is shown at the top, and the letters indicate the intermediate positions through which the presented ZEKE spectra were recorded. See text for discussion of the assignments. Asterisks and obeli (†) indicate accidental resonances and are discussed in Section III.B.

Figure 5: (a) Photoelectron spectrum recorded following the coherent excitation of the $9^1\ldots11^2\ldots29^2$ and $11^2\ldots9^1\ldots29^2$ eigenstates using ps laser pulses. The spectrum is shown at two time delays: the solid line denotes the spectrum recorded at a delay between the pump and probe pulses of 0 ps, while the dashed line denotes the spectrum recorded at 5 ps. The resolution is ~200 cm^{-1} and consequently a number of transitions may contribute to a feature – compare with the ZEKE spectra in Figure 4.

(b) Time variation of the 0^0 and 11^1 photoelectron bands as a function of the time delay between the excitation and ionization pulses following the coherent excitation of the $9^1\ldots11^2\ldots29^2$ and $11^2\ldots9^1\ldots29^2$ eigenstates using the ps laser pulses. The symbols indicate photoelectron intensities determined from the area of the relevant photoelectron band, while the lines are just to guide the eye.

Figure 6: (a) Variation of the intensity of the 0^0 band as a function of the time delay between the excitation and ionization lasers, following the coherent excitation of the $9^1\ldots11^2\ldots29^2$ and $11^2\ldots9^1\ldots29^2$ eigenstates using ps laser pulses. The dots are experimental intensities obtained by

scanning the delay stage, and the solid line is a fit to the empirical data – see text for details.(b) Fourier transform of the empirical data shown in (a). The two peaks observed correspond to energy separations between eigenstates – see text for further details.

Figure 7: An expanded view of the 860–970 cm^{-1} region of the REMPI spectrum shown in Figure 1 is shown at the top. A ZEKE spectra recorded via the $S_1\,18^2$ resonance is shown in (a), while traces (b)–(d) show ZEKE spectra recorded at the positions indicated by letters on the REMPI trace. See text for discussion of the assignments. Asterisks and obeli (†) indicate accidental resonances and are discussed in Section III.B.

Figure 8: An expanded view of the 1047–1063 cm^{-1} and 1105–1130 cm^{-1} regions of the REMPI spectrum shown in Figure 1 is presented at the top showing the bands that are used as intermediates in recording the ZEKE spectra presented. The letters on the REMPI trace indicate the intermediate positions through which the presented ZEKE spectra were recorded. See text for discussion of the assignments. Asterisks and obeli (†) indicate accidental resonances and are discussed in Section III.B.

Figure 9: An expanded view of the 1150–1195 cm^{-1} region of the REMPI spectrum shown in Figure 1 is presented at the top showing the bands that are used as intermediates in recording the ZEKE spectra presented. See text for discussion of the assignments. The REMPI band at 1155 cm^{-1} is a hot band and indicated by a red dot.

Figure 10: An expanded view of the 1202–1245 cm^{-1} region of the REMPI spectrum shown in Figure 1 is presented at the top showing the bands that are used as intermediates in recording the ZEKE spectra presented. See text for discussion of the assignments. Asterisks and obeli (†) indicate accidental resonances and are discussed in Section III.B.

Figure 11: An expanded view of the 1240–1292 cm^{-1} region of the REMPI spectrum shown in Figure 1 is presented at the top showing the bands that are used as intermediates in recording the ZEKE spectra presented; note that the 5^1 band (marked as X) is off scale – see Figure 1. See text for discussion of the assignments. Asterisks and obeli (†) indicate accidental resonances and are discussed in Section III.B.

Figure 1

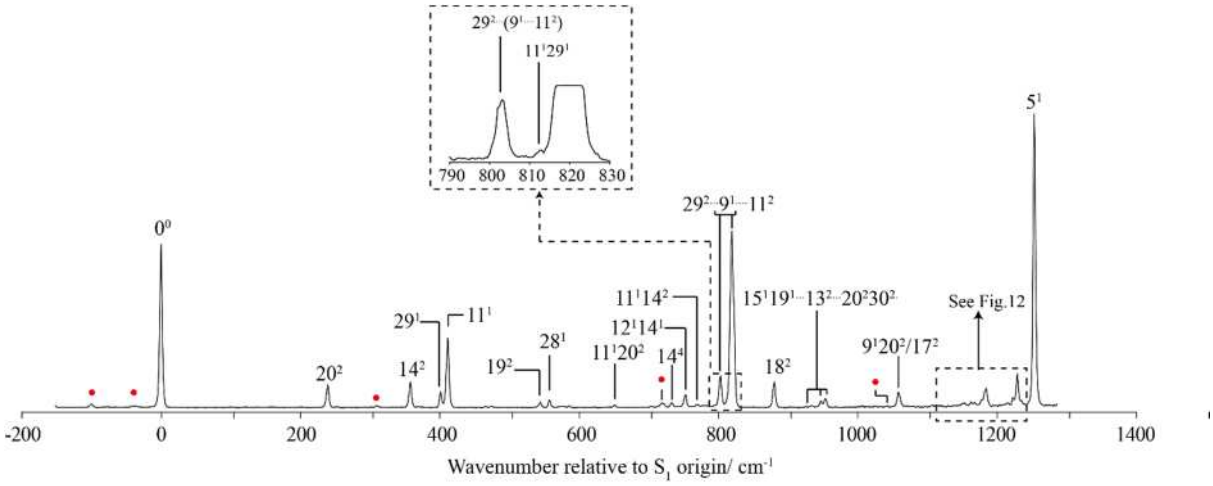
29^2 (9^1–11^2)
11^129^1
790 800 810 820 830
0^0
20^2
14^2
29^1
11^1
19^2
28^1
11^120^2
12^114^1
14^4
11^114^2
29^2–9^1–11^2
18^2
15^119^1–13^2–20^230^2
$9^120^2/17^2$
See Fig.12
5^1
-200 0 200 400 600 800 1000 1200 1400
Wavenumber relative to S_1 origin/ cm^{-1}

Figure 2

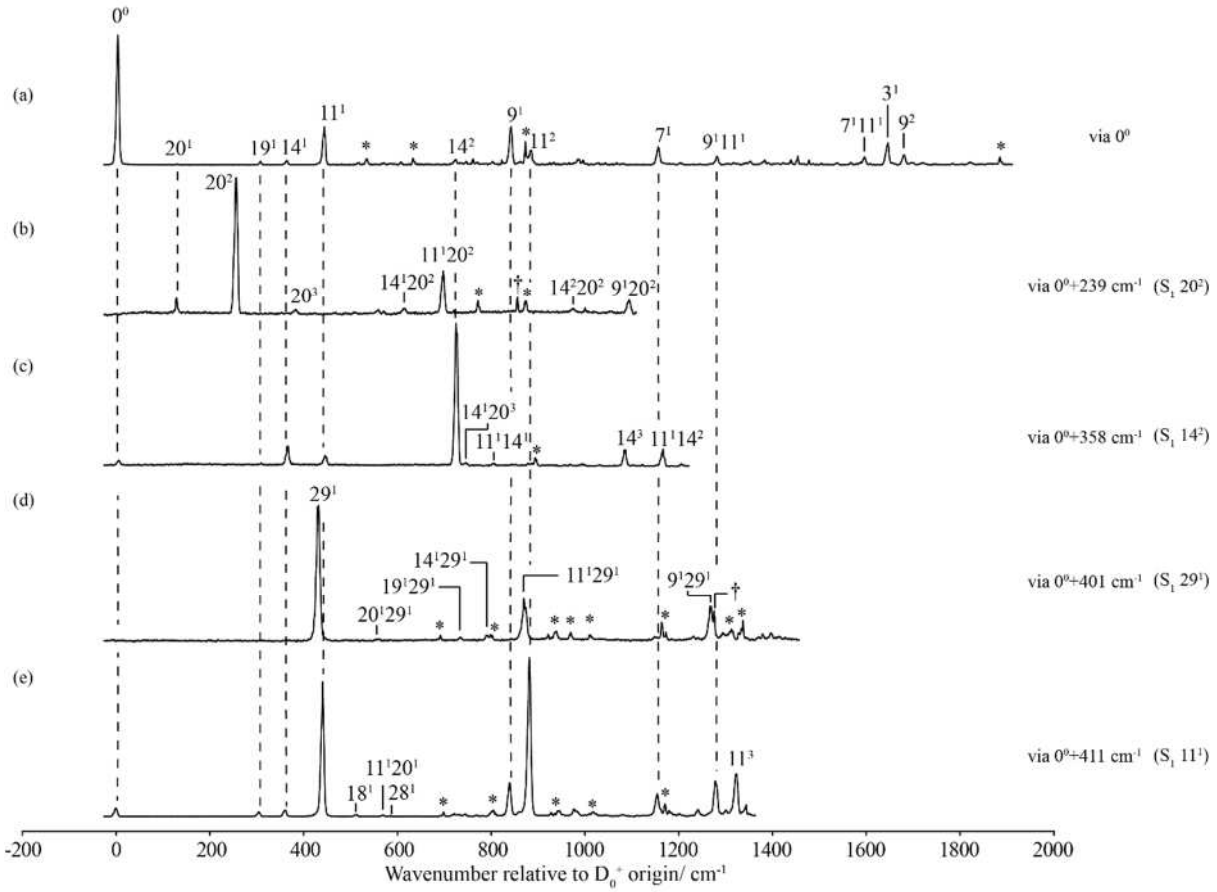
(a)
(b)
(c)
(d)
(e)
via 0⁰
via 0⁰+239 cm⁻¹ (S₁ 20²)
via 0⁰+358 cm⁻¹ (S₁ 14²)
via 0⁰+401 cm⁻¹ (S₁ 29¹)
via 0⁰+411 cm⁻¹ (S₁ 11¹)
Wavenumber relative to D₀⁺ origin/ cm⁻¹

Figure 3

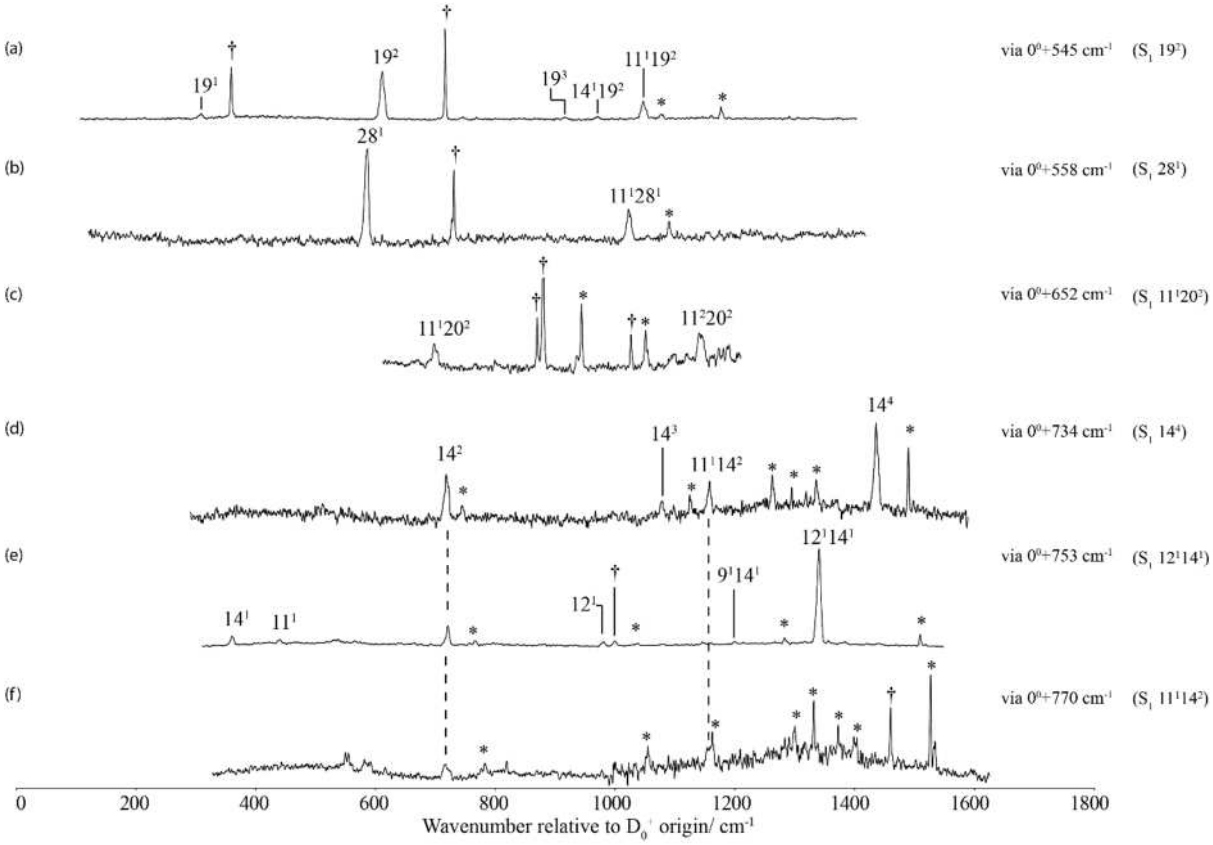
(a)
via 0^0+545 cm^{-1} (S_1 19^2)
19^1
19^2
19^3
$14^1 19^2$
$11^1 19^2$
(b)
via 0^0+558 cm^{-1} (S_1 28^1)
28^1
$11^1 28^1$
(c)
via 0^0+652 cm^{-1} (S_1 $11^1 20^2$)
$11^1 20^2$
$11^2 20^2$
(d)
via 0^0+734 cm^{-1} (S_1 14^4)
14^2
14^3
$11^1 14^2$
14^4
(e)
via 0^0+753 cm^{-1} (S_1 $12^1 14^1$)
14^1
11^1
12^1
$9^1 14^1$
$12^1 14^1$
(f)
via 0^0+770 cm^{-1} (S_1 $11^1 14^2$)
0
200
400
600
800
1000
1200
1400
1600
1800
Wavenumber relative to D_0^+ origin/ cm^{-1}

Figure 4

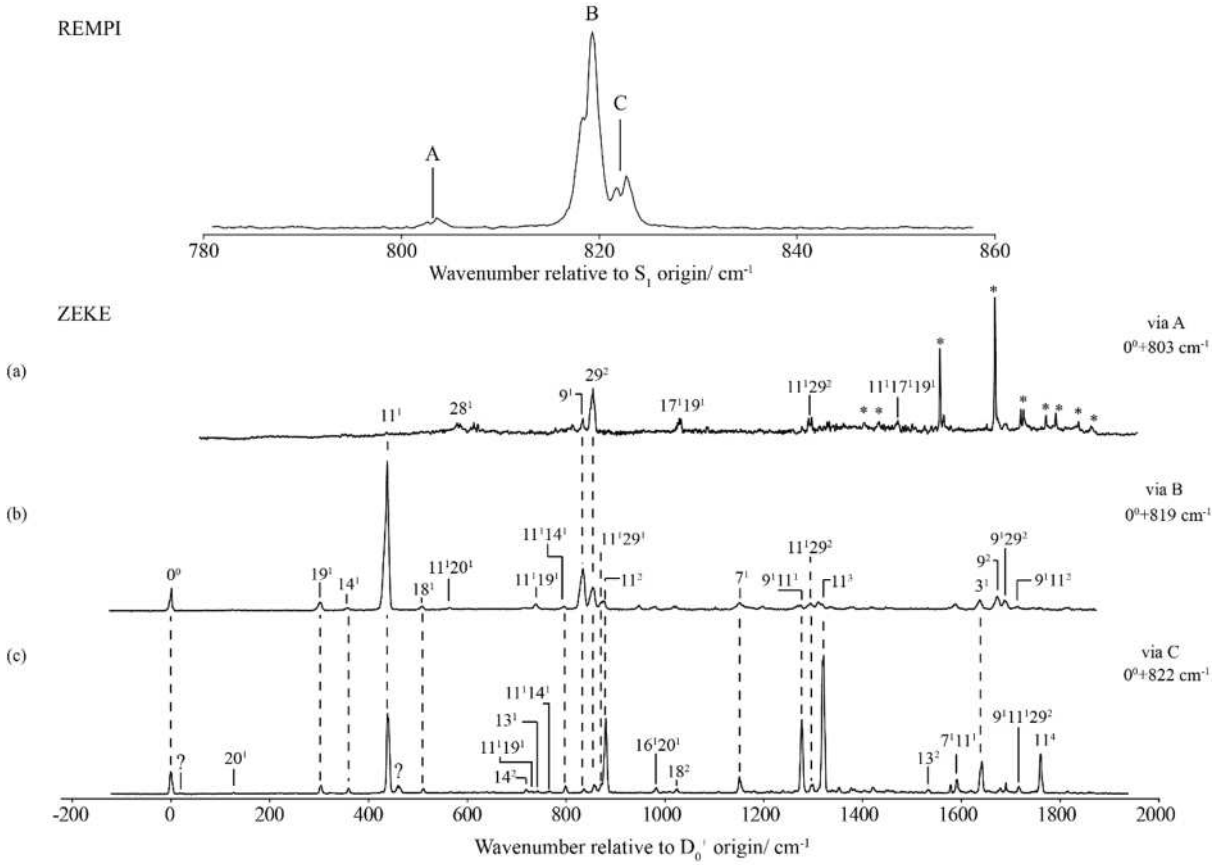
REMPI
A
B
C
780
800
820
840
860
Wavenumber relative to S1 origin/ cm-1
ZEKE
(a)
via A
0⁰+803 cm-1
11¹
28¹
9¹
29²
17¹19¹
11¹29²
11¹17¹19¹
(b)
via B
0⁰+819 cm-1
0⁰
19¹
14¹
18¹
11¹20¹
11¹14¹
11¹19¹
11¹29¹
11²
7¹
9¹11¹
11¹29²
11³
9²
3¹
9¹29²
9¹11²
(c)
via C
0⁰+822 cm-1
?
20¹
?
11¹14¹
13¹
11¹19¹
14²
16¹20¹
18²
13²
7¹11¹
9¹11¹29²
11⁴
-200
0
200
400
600
800
1000
1200
1400
1600
1800
2000
Wavenumber relative to D0¹ origin/ cm-1

Figure 5

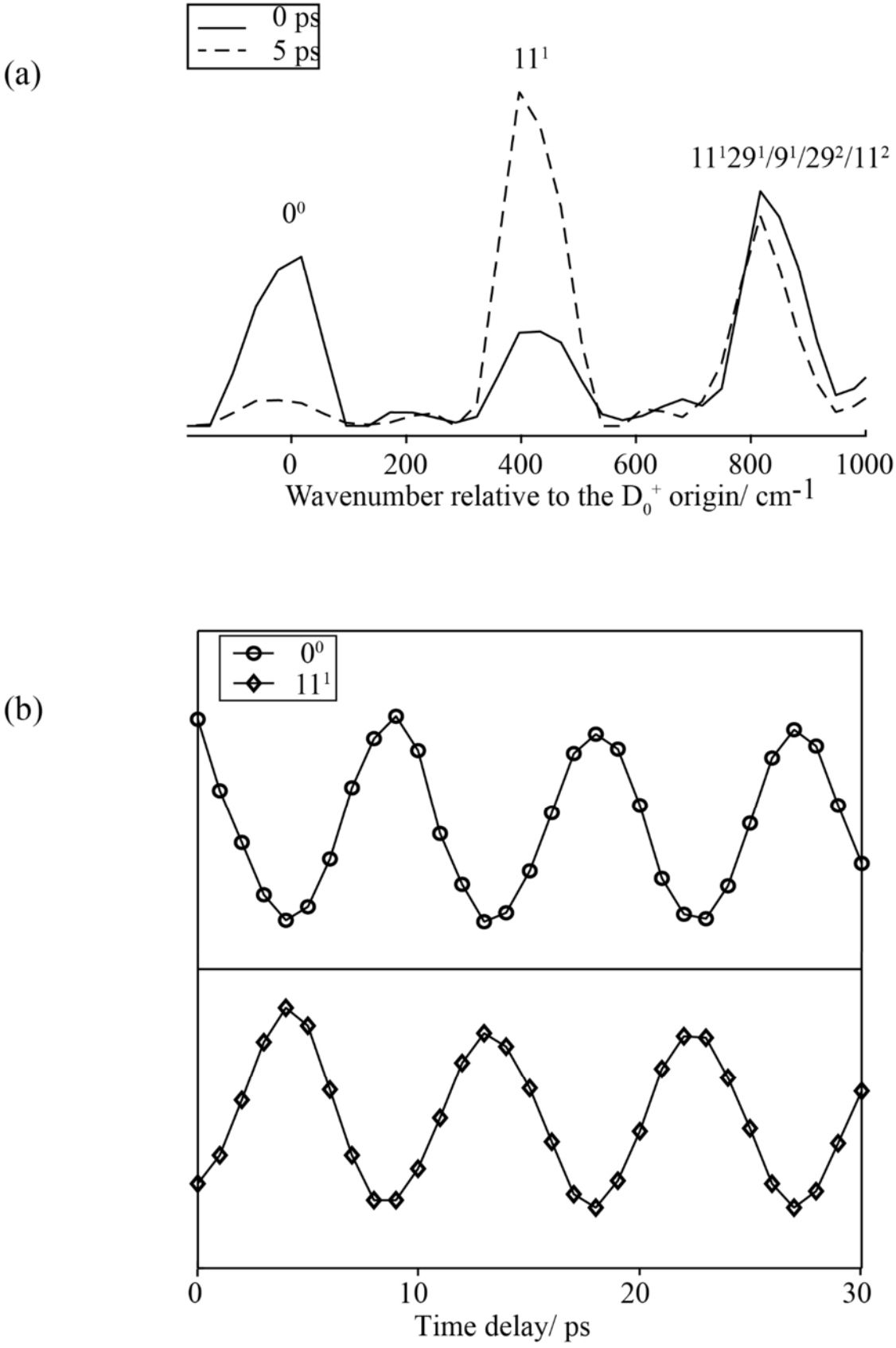
(a)
0 ps
5 ps
11^1
$11^129^1/9^1/29^2/11^2$
0^0
0
200
400
600
800
1000
Wavenumber relative to the D_0^+ origin/ cm^{-1}
(b)
0^0
11^1
0
10
20
30
Time delay/ ps

Figure 6

(a)

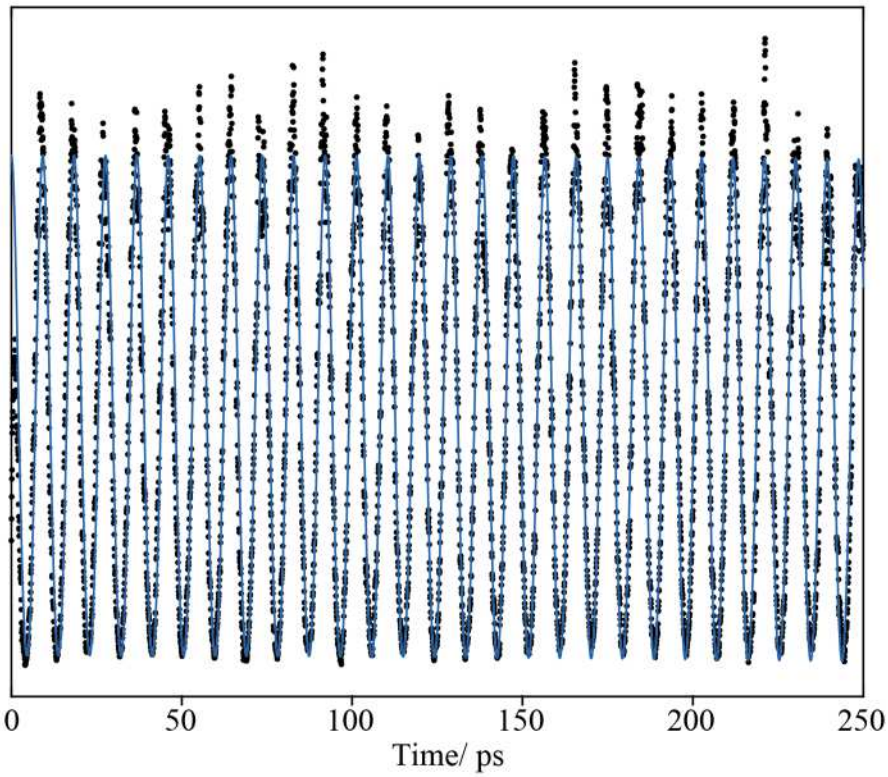

(b)

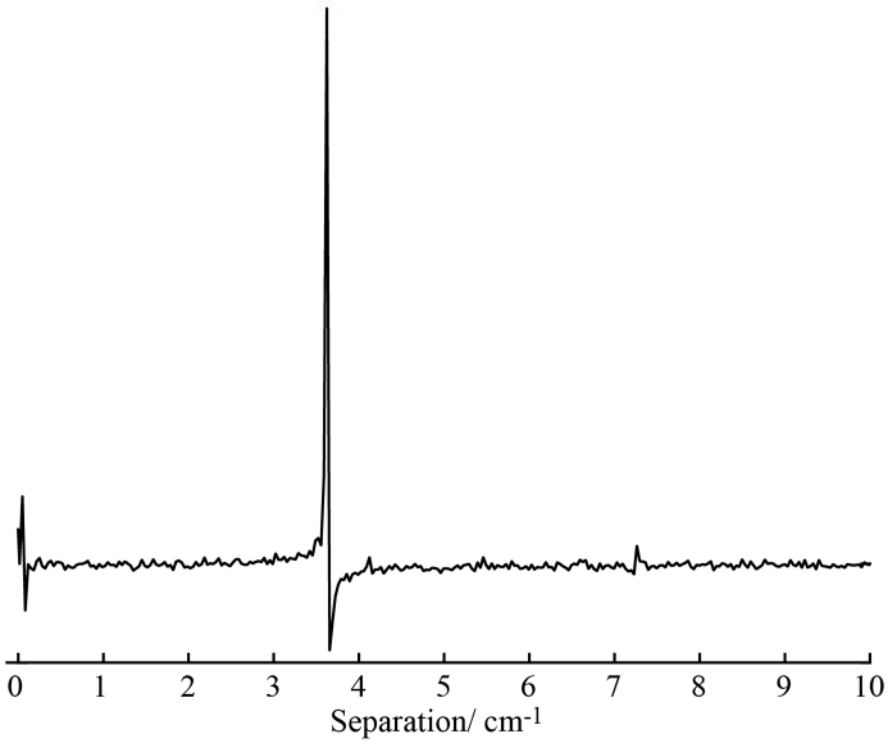

Figure 7

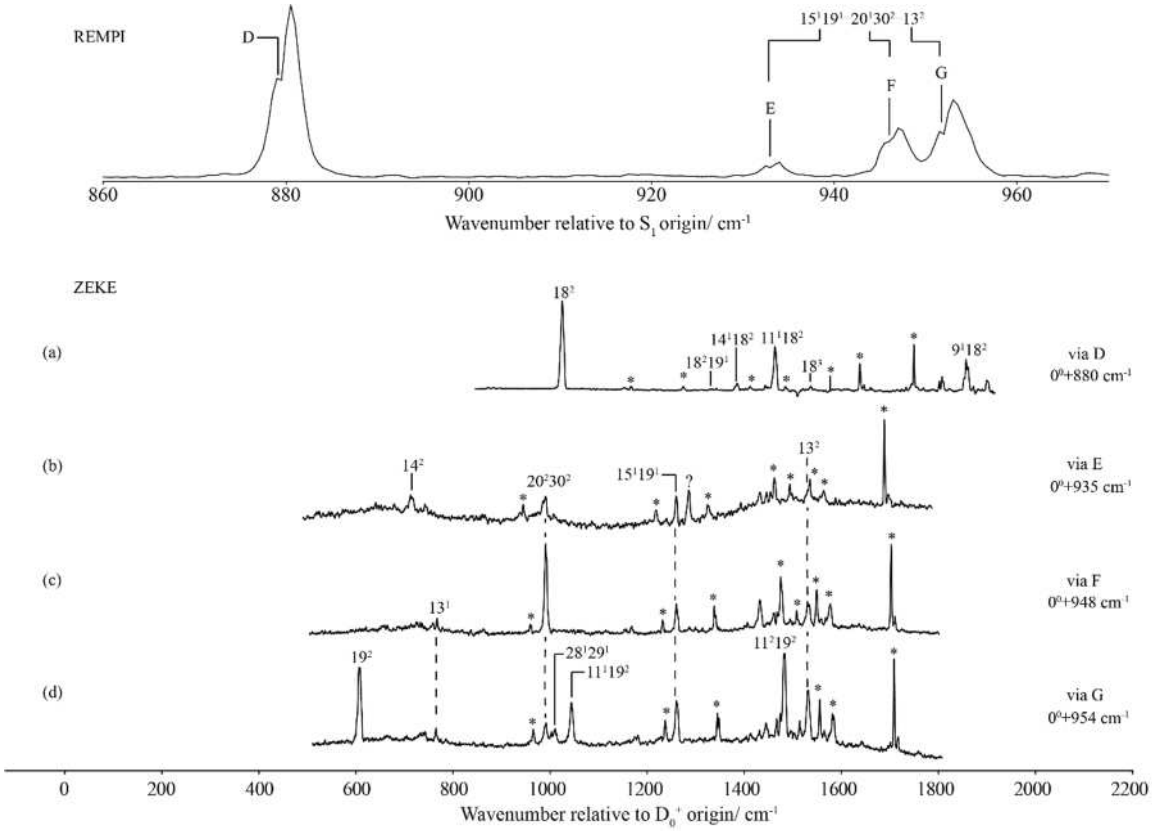
REMPI
D
E
F
G
$15^1 19^1$ $20^1 30^2$ 13^2
860
880
900
920
940
960
Wavenumber relative to S_1 origin/ cm^{-1}
ZEKE
(a)
(b)
(c)
(d)
18^3
$14^1 18^2$ $11^1 18^2$
$18^2 19^1$
18^3
$9^1 18^2$
via D
0^0+880 cm^{-1}
14^2
$20^2 30^2$
$15^1 19^1$
?
13^2
via E
0^0+935 cm^{-1}
13^1
via F
0^0+948 cm^{-1}
19^2
$28^1 29^1$
$11^1 19^2$
$11^2 19^2$
via G
0^0+954 cm^{-1}
0
200
400
600
800
1000
1200
1400
1600
1800
2000
2200
Wavenumber relative to D_0^+ origin/ cm^{-1}

Figure 8

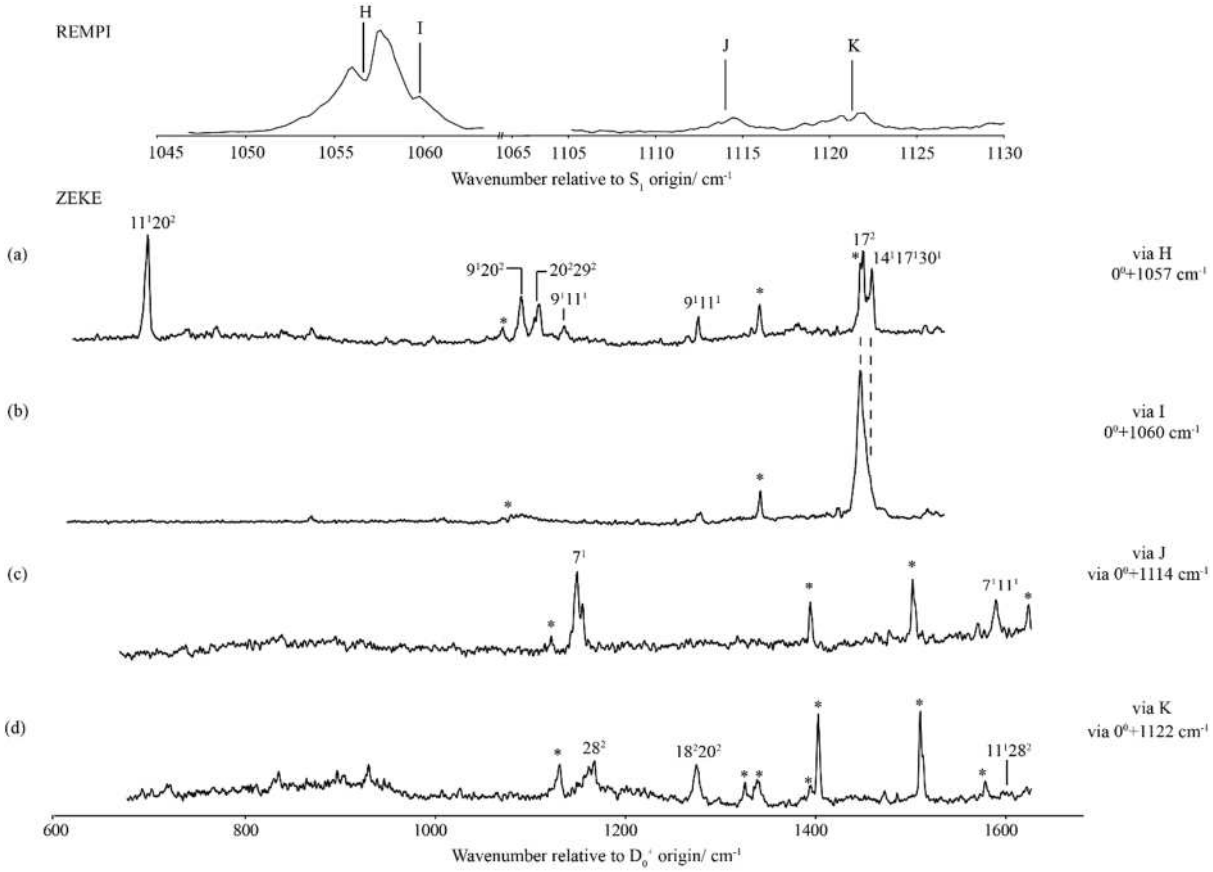
REMPI
H
I
J
K
1045
1050
1055
1060
1065
1105
1110
1115
1120
1125
1130
Wavenumber relative to S1 origin/ cm-1
ZEKE
(a)
11¹20²
9¹20²
20²29²
9¹11¹
9¹11¹
17²
14¹17¹30¹
via H
0⁰+1057 cm-1
(b)
via I
0⁰+1060 cm-1
(c)
7¹
7¹11¹
via J
via 0⁰+1114 cm-1
(d)
28²
18²20²
11¹28²
via K
via 0⁰+1122 cm-1
600
800
1000
1200
1400
1600
Wavenumber relative to D0+ origin/ cm-1

Figure 9

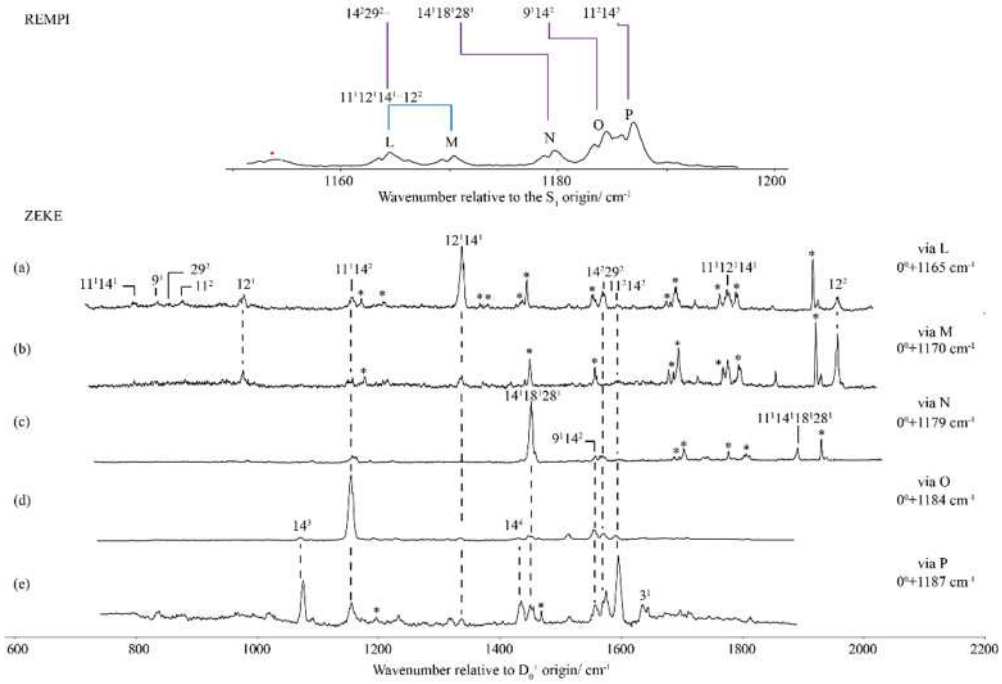
REMPI
L
M
N
O
P
1160
1180
1200
Wavenumber relative to the S1 origin/ cm-1
ZEKE
(a)
(b)
(c)
(d)
(e)
via L
via M
via N
via O
via P
600
800
1000
1200
1400
1600
1800
2000
2200
Wavenumber relative to D0+ origin/ cm-1

Figure 10

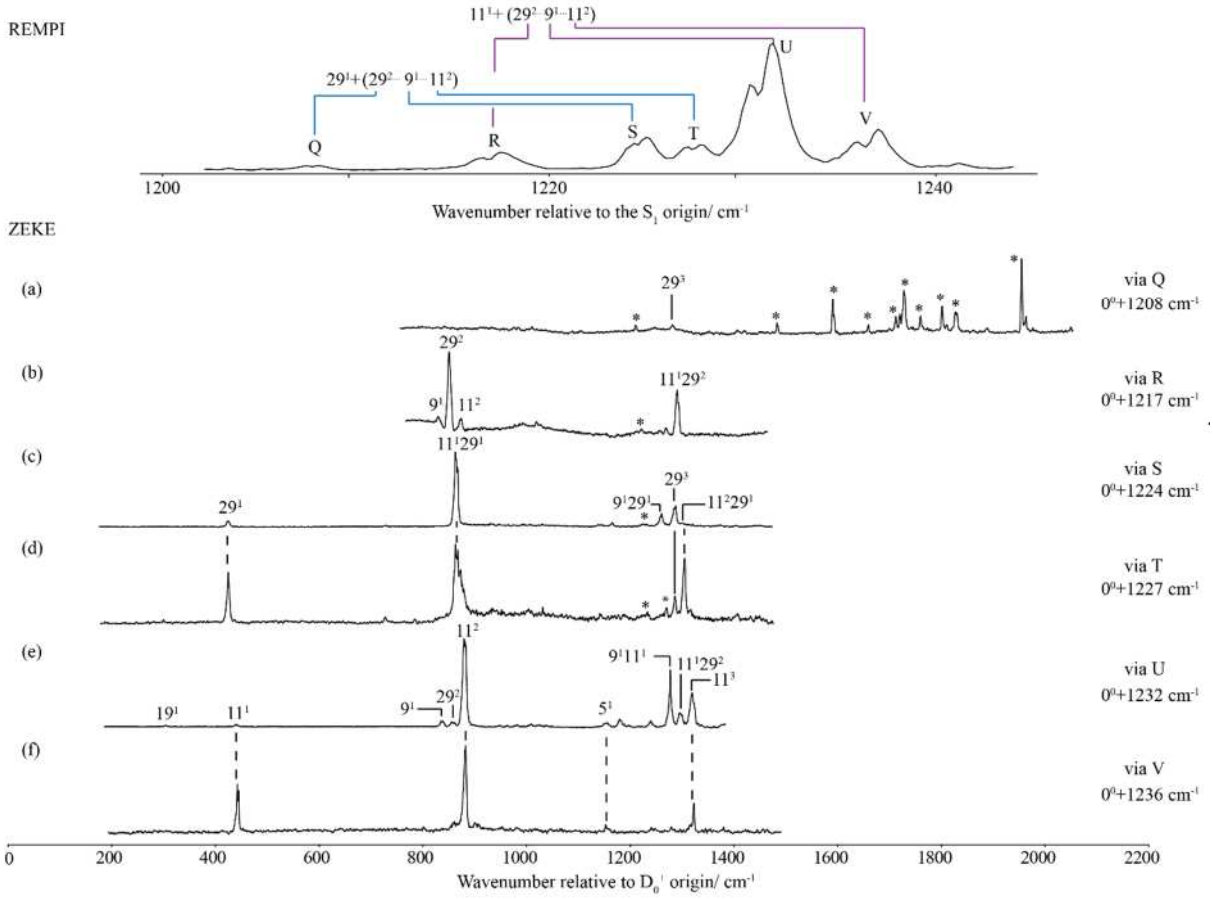
REMPI
$11^1+(29^2\ 9^1\ 11^2)$
$29^1+(29^2\ 9^1\ 11^2)$
Q
R
S
T
U
V
1200
1220
1240
Wavenumber relative to the S_1 origin/ cm^{-1}
ZEKE
(a)
29^3
via Q
$0^0+1208\ cm^{-1}$
(b)
29^2
9^1
11^2
11^129^2
via R
$0^0+1217\ cm^{-1}$
(c)
11^129^1
29^1
29^3
9^129^1
11^229^1
via S
$0^0+1224\ cm^{-1}$
(d)
via T
$0^0+1227\ cm^{-1}$
(e)
11^2
9^111^1
11^129^2
11^3
19^1
11^1
9^1
29^2
5^1
via U
$0^0+1232\ cm^{-1}$
(f)
via V
$0^0+1236\ cm^{-1}$
0
200
400
600
800
1000
1200
1400
1600
1800
2000
2200
Wavenumber relative to D_0^+ origin/ cm^{-1}

Figure 11

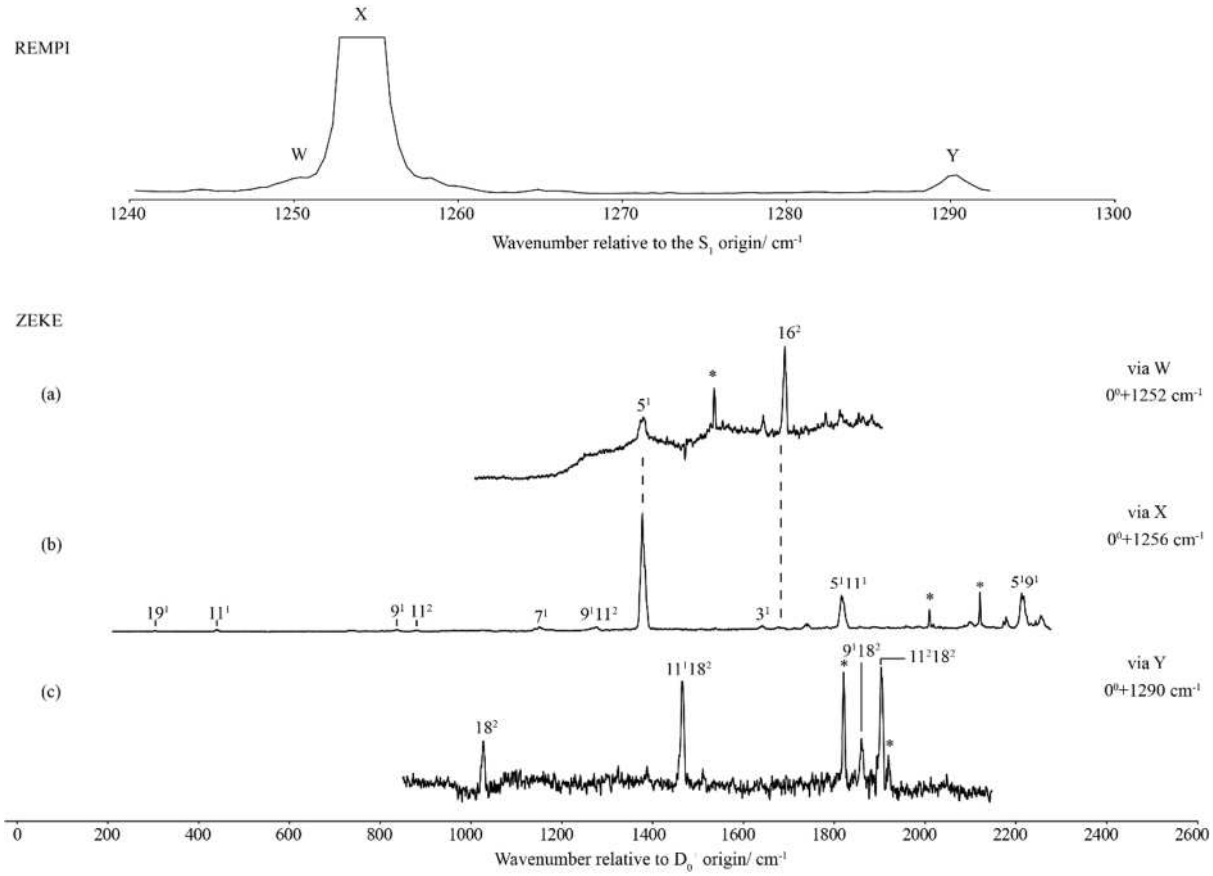
REMPI
X
W
Y
1240
1250
1260
1270
1280
1290
1300
Wavenumber relative to the S1 origin/ cm-1
ZEKE
(a)
(b)
(c)
via W
0⁰+1252 cm-1
via X
0⁰+1256 cm-1
via Y
0⁰+1290 cm-1
16²
5¹
19¹
11¹
9¹ 11²
7¹
9¹11²
3¹
5¹11¹
5¹9¹
11¹18²
9¹18²
11²18²
18²
0
200
400
600
800
1000
1200
1400
1600
1800
2000
2200
2400
2600
Wavenumber relative to D0 origin/ cm-1

References

[1] C. D. Cooper, J. Chem. Phys. **22**, 503 (1954).

[2] M. J. Robey and E. W. Schlag, Chem. Phys. **30**, 9 (1978).

[3] R. A. Coveleskie and C. S. Parmenter, J. Molec. Spectrosc. **86**, 86 (1981).

[4] A. E. W. Knight and S. H. Kable, J. Chem. Phys. **89**, 7139 (1988). Note that this work includes a significant number of further spectra and comments as part of the Supplementary Information.

[5] Q. Ju, C. S. Parmenter, T. A. Stone, and Z.-Q. Zhao, Isr. J. Chem. **37**, 379 (1997).

[6] E. Sekreta, K. S. Viswanathan, and J. P. Reilly, J. Chem. Phys. **90**, 5349 (1989).

[7] S. M. Bellm and K. L. Reid, Chem. Phys. Lett. **395**, 253 (2004).

[8] D. Rieger, G. Reiser, K. Müller-Dethlefs, and E. W. Schlag, J. Phys. Chem. **96**, 12 (1992).

[9] G. Reiser, D. Rieger, T. G. Wright, K. Müller-Dethlefs, and E. W. Schlag, J. Phys. Chem. **97**, 4335 (1993).

[10] G. Lembach and B. Brutschy, J. Phys. Chem. A, **102**, 6068 (1998).

[11] C. H. Kwon, H. L. Kim, and M. S. Kim, J. Chem. Phys. **118**, 6327 (2003).

[12] V. E. Bondybey, T. A. Miller, and J. H. English, J. Chem. Phys. **72**, 2193 (1980).

[13] Y. Tsuchiya, M. Fujii, and M. Ito, J. Chem. Phys. **90**, 6965 (1989).

[14] Y. Tsuchiya, M. Fujii, and M. Ito, Chem. Phys. Lett. **168**, 173 (1990).

[15] S.-Y. Yu and M.-B. Huang, J. Molec. Struct. THEOCHEM **822**, 48 (2007).

[16] D. Boyall and K. L. Reid, Chem. Soc. Rev. **26**, 223 (1997).

[17] K. L. Reid, Int. Rev. Phys. Chem. **27**, 607 (2008).

[18] J. A. Davies, A. M. Green, A. M Gardner, C. D. Withers, T. G. Wright, and K. L. Reid, Phys. Chem. Chem. Phys. **16**, 430 (2014).

[19] S. D. Gamblin, S. E. Daire, J. Lozeille, and T. G. Wright, Chem. Phys. Lett. **325**, 232 (2000).

[20] V. L. Ayles, C. J. Hammond, D. E. Bergeron, O. J. Richards, and T. G. Wright, J. Chem. Phys. **126**, 244304 (2007).

[21] X. Zhang, J. M. Smith, and J. L. Knee, J. Chem. Phys. **97**, 2843 (1992).

[22] J. A. Davies, A. M. Green, and K. L. Reid, Phys. Chem. Chem. Phys. **12**, 9872 (2010).

[23] J. Midgley, J. A. Davies, and K. L. Reid, J. Phys. Chem. Lett. **5**, 2482 (2014).

[24] J. Midgley, J. A. Davies, and K. L. Reid, J. Chem. Phys. **139**, 117101 (2013).

[25] A. Andrejeva, A. M. Gardner, W. D. Tuttle, and T. G. Wright, J. Molec. Spectrosc. **321**, 28 (2016).

[26] W. D. Tuttle, A. M. Gardner, K. B. O'Regan, W. Malewicz, and T. G. Wright, J. Chem. Phys. **146**, 124309 (2017).

[27] W. D. Tuttle, A. M. Gardner, L. E. Whalley, and T. G. Wright, J. Chem. Phys. **146**, 244310 (2017).

[28] T. Cvitaš and J. M. Hollas, Mol. Phys. **18**, 793 (1970).

[29] W. D. Tuttle, A. M. Gardner, and T. G. Wright, Chem. Phys. Lett. **684**, 339 (2017).

[30] R. S. Mulliken, J. Chem. Phys. **23**, 1997 (1955).

[31] G. Herzberg, *Molecular Spectra and Molecular Structure II. Infrared and Raman Spectra of Polyatomic Molecules* (Krieger, Malabar, 1991).

[32] E. B. Wilson, Jr, Phys. Rev. **45**, 706 (1934).

[33] G. Varsányi, *Assignments of the Vibrational Spectra of Seven Hundred Benzene Derivatives* (Wiley, New York, 1974).

[34] M. Fujii, T. Kakinuma, N. Mikami, and M. Uto, Chem. Phys. Lett. **127**, 297 (1986).

[35] D. J. Kemp, L. E. Whalley, W. D. Tuttle, A. M. Gardner, B. T. Speake, and T. G. Wright, *Phys. Chem. Chem. Phys.* **20**, 12503 (2018).

[36] T. G. Blease, R. J. Donovan, P. R. R. Langridge-Smith, and T. R. Ridley, Laser Chem. **9**, 241 (1988).

[37] Z.-Q. Zhao and C. S. Parmenter, Ber. Bunsenges. Phys. Chem. **99**, 536 (1995).

[38] J. A. Davies and K. L. Reid, Phys. Rev. Lett. **109**, 193004 (2012).

[39]W. D. Tuttle, A. M. Gardner, L. E. Whalley, D. J. Kemp, and T. G. Wright, Phys. Chem. Chem. Phys. DOI: 10.1039/C8CP02757A.

[40] A. M Gardner, W. D. Tuttle, L. E. Whalley, and T. G. Wright, Chem. Sci. **9**, 2270 (2018).

[41] J. Long, C. Qin, Y. Liu, S. Zhang, and B. Zhang, Phys. Rev. A **84**, 063409 (2011).

[42] N. T. Whetton and W. D. Lawrance, J. Phys. Chem. **93**, 5377 (1989).

[43] I. Pugliesi, N. M. Tonge, and M. C. R. Cockett, J. Chem. Phys. **129**, 104303 (2008).

[44] See, for example, W. A. Chupka, J. Chem. Phys. **98**, 4529 (1993).

[45] G. J. Rathbone, E. D. Poliakoff, J. D. Bozek, and R. R. Lucchese, Can. J. Chem. **82**, 1043 (2004).

[46] J. S. Miller, E. D. Poliakoff, T. F. Miller III, A. P. Natalense, and R. R. Lucchese, J. Chem. Phys. **114**, 4496 (2001).

[47] E. D. Poliakoff and R. R. Lucchese, Phys. Scr. **74**, C71 (2006).

[48] G. A. Garcia, H. Dossmann, L. Nahon, S. Daly, and I. Powis, ChemPhysChem, **18**, 500 (2017).